Title

Paths to adaptation under fluctuating nitrogen starvation: The spectrum of adaptive mutations in *Saccharomyces cerevisiae* is shaped by transposons and microhomology-mediated recombination

Authors

Michelle Hays[1]*, Katja Schwartz[1]*, Danica T. Schmidtke[2], Dimitra Aggeli[1,3], Gavin Sherlock[1]

*Equal contribution

Corresponding author: G.S. (Email: gsherloc@stanford.edu)

Departments of [1]Genetics and [2]Microbiology and Immunology, Stanford University School of Medicine, Stanford, CA 94305

[3]Current address: Department of Biological Sciences, Lehigh University, Bethlehem, PA 18015

Abstract

There are many mechanisms that give rise to genomic change: while point mutations are often emphasized in genomic analyses, evolution acts upon many other types of genetic changes that can result in less subtle perturbations. Changes in chromosome structure, DNA copy number, and novel transposon insertions all create large genomic changes, which can have correspondingly large impacts on phenotypes and fitness. In this study we investigate the spectrum of adaptive mutations that arise in a population under consistently fluctuating nitrogen conditions. We specifically contrast these adaptive alleles and the mutational mechanisms that create them, with mechanisms of adaptation under batch glucose limitation and constant selection in low, non-fluctuating nitrogen conditions. We observe that retrotransposon activity accounts for a substantial number of adaptive events, along with microhomology-mediated mechanisms of insertion, deletion, and gene conversion. In addition to loss of function alleles, which are often exploited in genetic screens, we identify adaptive gain of function alleles and alleles acting through as-of-yet unclear mechanisms. Taken together, our findings emphasize that *how* selection (fluctuating vs. non-fluctuating) is applied also shapes adaptation, just as the selective pressure (nitrogen vs. glucose) does itself. Fluctuating environments can activate different mutational mechanisms, shaping adaptive events accordingly. Experimental evolution, which allows a wider array of adaptive events to be assessed, is thus a complementary approach to both classical genetic screens and natural variation studies to characterize the genotype-to-phenotype-to-fitness map.

Introduction

Genomic changes often underlie phenotypic variation and population evolution. To understand phenotypic variation, genetic screens can identify relevant loci, but are often limited in the types of genomic changes they explore. For example, screens often use mutagens with specific mutational mechanisms, or collections of deletion mutants. Alternatively, comparative genomics can establish which changes have previously arisen and survived, but linking such changes to fitness and adaptation can be challenging. By contrast, experimental evolution can reveal how organisms adapt under specific selective pressures, revealing the most fit and/or frequent beneficial mutations (e.g. Jacquier et al. 2013; Lang et al. 2013; Hong and Gresham 2014; Payen et al. 2016; Venkataram et al. 2016; Good et al. 2017). The mutational types that arise during experimental evolution are not limited to those typically isolated from genetic screens, but rather reflect the mutational mechanisms active in a population experiencing a selective pressure of interest. The relative rates and effects of different mutagenic mechanisms differ greatly in yeast, with single nucleotide polymorphisms (SNPs) arising at ~10^{-10} per nucleotide per generation (Lang and Murray 2008), while aneuploidy, for example, has been observed at ~10^{-4} per generation (Zhu et al. 2014) (though it can vary greatly between chromosomes and genetic backgrounds (Kumaran et al. 2013)) and affects hundreds of genes at a time. Other mutagenic mechanisms, such as transposition, recombination-driven gene conversion, loss of heterozygosity, and structural rearrangements may also give rise to adaptive events unique to those mechanisms and can also occur during experimental evolution. Therefore, experimental evolution is an especially useful tool to understand how genome changes facilitate adaptation. By profiling the target loci at which adaptation occurs, the mutagenic mechanisms that create those changes, and the specific adaptive alleles that arise, agnostic to gain or loss of function, a more complete view of the genotype-to-phenotype map can emerge. Thus, experimental

evolution complements, rather than simply reproduces, findings obtained through other types of genetic studies.

Some stress conditions are linked to increases in specific mutagenic mechanisms and stress-induced genomic instability may even improve evolvability of organisms (Galhardo et al. 2007). Populations under stress may therefore sample more genotypic and phenotypic states, aiding population survival in environments for which ancestors were ill-adapted. Transposons are mobilized in many species in response to stress (e.g. Chen et al. 2003; Hashida et al. 2003; Hashida et al. 2006; Sehgal et al. 2007; Chenais et al. 2012; Jardim et al. 2015; Miousse et al. 2015; Esnault et al. 2019; Fouche et al. 2020; Roquis et al. 2021), including in *Saccharomyces cerevisiae* (Bradshaw and McEntee 1989; Wilke and Adams 1992; Scholes et al. 2003; Sacerdot et al. 2005; Todeschini et al. 2005; Servant et al. 2008; Stoycheva et al. 2010; Servant et al. 2012), leading to an increase in transposon-driven mutagenesis. *S. cerevisiae* has five families of Long Terminal Repeat (LTR) retrotransposons: Ty1 - Ty5 (Rowley 2017; Bonnet and Lesage 2021). Ty1 and Ty2 are closely related and are the two most abundant families in the reference genome. Ty1 transcription increases under DNA damaging conditions (Bradshaw and McEntee 1989), extreme adenine starvation (Servant et al. 2008), filamentous growth (as a result of carbon or nitrogen starvation; Morillon et al. 2000), and telomere shortening (Scholes et al. 2003). Newly integrated Ty copies can interrupt host gene coding sequences or alter host gene regulation, causing increased, decreased or even constitutive activation of neighboring ORFs. This regulatory capacity arguably makes transposon mutagenesis more powerful for driving host genome evolution, and possibly even determining evolvability itself, than, for example, point mutations. Genomic variation also arises comparatively frequently through several microhomology mediated mechanisms (Dan et al. 2021). These events, such as microhomology-mediated translocations, duplications, deletions, and gene conversion events, cause variants to arise more frequently specifically at sites of short sequences found tandemly

repeated within a genome (Dan et al. 2021). This increased frequency of site-specific mutation could influence population evolvability and adaptation, disproportionately impacting the evolution of genomic regions containing microhomology.

Laboratory-directed microbial evolution experiments allow investigation of how selective pressures shape genome evolution and most often make use of either serial transfer or continuous culture (Long et al. 2015; Voordeckers and Verstrepen 2015; Cooper 2018). The selective pressure can come from nutrient limitation, the presence of an inhibitor (such as an antibiotic) or a restrictive environmental condition (e.g. temperature). In serial batch transfer evolutions, populations are iteratively passaged into fresh media, leading to regular environmental fluctuations. By contrast, in chemostat or turbidostat growth, continuous flow into the culture chamber of fresh medium and outflow of spent medium/cells produces a constant environment (Gresham and Dunham 2014). This fundamental difference between fluctuating vs. constant selective pressure can drive different means of genome evolution: the rates that some classes of mutations arise may differ between these approaches, and the relative fitness of evolved alleles may differ as well.

S. cerevisiae's adaptation to glucose limitation has been well-studied in both chemostat and serial transfer conditions and each results in different adaptive mutational spectra (Gresham et al. 2008; Kao and Sherlock 2008; Kvitek and Sherlock 2013; Lang et al. 2013; Venkataram et al. 2016). Continuous culture in limiting glucose predominantly selects for mutants with more rapid glucose uptake, such as amplifications of the *HXT* glucose transporters (Brown et al. 1998), as well as lineages that fail to mount starvation stress responses (Kvitek and Sherlock 2013). By contrast, in fluctuating glucose conditions, self-diploidization and point mutations in the Ras and TOR pathways predominate (Venkataram et al. 2016), the latter often resulting in a shorter lag phase (Li et al. 2018).

Like carbon, nitrogen is an essential nutrient for yeast survival. Nitrogen sensing and uptake also uses a complex signaling network with several feedback loops and points of self-regulation. Nitrogen-sensing impacts many other cell states as well, such as initiation of catabolic programs to scavenge nutrients from within and changes in growth programs such as filamentous growth and biofilm formation. Just as yeast favors glucose as a carbon source, it also preferentially favors different nitrogen sources (see Hofman-Bang 1999). Depending on environmental nitrogen sources available, yeast may import nitrogen through substrate-specific transporters (such as Mep1/3 and Mep2 for ammonia or Gnp1 for glutamine) or through more general transporters (such as the general amino acid permease - Gap1), or a combination thereof (Andre 1995; Regenberg et al. 1999; Magasanik and Kaiser 2002; Garrett 2008). The nitrogen catabolite repression (NCR) and retrograde response pathways facilitate regulation and usage of different nitrogen sources (see Cooper 2002; Conrad et al. 2014); both of these pathways involve TOR signaling, and NCR exhibits self-regulation. For example, Gat1 is a central regulator of NCR and participates in several feedback loops, including self-activation (Coffman et al. 1997). Gat1 is also required as a coactivator along with Gln3 at many NCR promoters. Additionally, NCR repressors Gzf3 and Dal80 function by interfering with Gat1 binding (including competition at the *GAT1* promoter), *GAT1* expression and Gat1 cellular localization (Georis et al. 2009).

Previously, experimental evolution of *S. cerevisiae* under constant nitrogen limitation demonstrated adaptive amplification of transporter genes associated with the specific nitrogen sources available. For example, the *GAP1* transporter gene has been observed to amplify in glutamine-limited chemostats via several mechanisms, including extrachromosomal circle formation facilitated by recombination between flanking LTRs (Gresham et al. 2010) and ODIRA (Lauer et al. 2018; Spealman et al. 2020). *DUR3* is amplified under urea limitation, *PUT4* under

proline limitation, *DAL4* under allantoin and *MEP2* under ammonium limitation respectively (Hong and Gresham 2014; Gresham and Hong 2015). Although the identities of the transporters amplified were dependent upon the nitrogen source available, permease amplification was frequently observed as a general class of adaptation. Conversely, loss of unutilized transporters can also be beneficial under continuous selection conditions (Hong and Gresham 2014; Lauer et al. 2018).

We set out to determine if, as was observed in adaption to glucose limitation, different classes of mutational mechanisms give rise to different modes of adaptation under fluctuating nitrogen limitation as compared to constant limitation. The relative complexity of regulation, pathway feedback and pleiotropy of nitrogen signaling may give rise to a distinct adaptive spectrum under fluctuating conditions that vary between low and zero nitrogen during the growth cycle. This fluctuating nitrogen condition provides an interesting case for comparison of adaptive mutational spectra, contrasting adaptation to limiting nutrients (glucose vs. nitrogen), and also constant vs. fluctuating conditions. These comparisons provide insight into how the application of selection (constant vs. fluctuating) shapes available adaptive routes and their relative fitness, as well as how the genetic architecture of a trait (nitrogen vs. carbon sensing) influences the spectrum of beneficial mutations.

Previously, we analyzed the population dynamics of prototrophic *S. cerevisiae* evolved under nitrogen-limited conditions by serial transfer, with ammonium as the limiting source of nitrogen (Blundell et al. 2019). We noted an initial increase in adaptive single-mutants, followed by a crash in population diversity due to clonal interference as a result of rapid expansion of highly beneficial double-mutants. Here, we more deeply explore the specific mechanisms underlying adaptation to nitrogen limitation, focusing on recurrently mutated loci and the different mutational classes that give rise to these adaptive alleles. We identify six loci that are often

targets of selection specifically under fluctuating nitrogen limitation where cells experience transient total nitrogen starvation. This suggests that mutation of these loci leads to the greatest fitness increases and/or that these loci are most easily and frequently mutated. In addition to SNPs and small indels, we observe several adaptive alleles that result from microhomology-mediated insertion, deletion or gene conversion, and multiple alleles that result from Ty insertions. This is in contrast to others' results under continuous growth conditions, where these classes of mutations are rarely observed and different loci are found most frequently mutated. While many of our identified adaptive alleles are likely loss of function mutants, we also identify putative gain of function mutations, again emphasizing the utility of experimental evolution for exploring the breadth and depth of adaptive alleles and the mechanisms that birth them.

Results:

Summary of nutrient-limited evolution experiments and lineage tracking

We previously evolved yeast by serial transfer under both glucose and nitrogen limitation (Levy et al. 2015; Blundell et al. 2019), using lineage tracking by barcode sequencing to identify adaptive lineages and to estimate fitness. Evolved clones were previously isolated for fitness validation and whole genome sequencing; briefly, ~5,000 clones were isolated from generations 88 and 192 (from glucose and nitrogen limitation respectively), their barcodes identified, and their ploidy was determined using a benomyl based assay as described (Venkataram et al. 2016; see Methods).

Sequencing of evolved clones from nitrogen limitation

To identify the underlying adaptive mutations, we whole-genome sequenced 345 clones with unique barcodes isolated from generation 192 of the nitrogen-limited evolution. These clones were selected based on the previously characterized barcode frequencies and their estimated

fitness during the evolution itself and were expected to include both neutral and adaptive clones. For diploids, we only sequenced those with estimated fitness greater than diploidy alone would provide. We analyzed the data for SNPs, small indels, and *de novo* transposition events; sequenced clones contained zero to five SNPs/indels and zero to nine Ty insertions (see Methods). To determine which of the observed mutations are likely adaptive, we looked for genomic loci that were recurrently mutated and whether these mutations correlated with reproducible fitness increases by fitness remeasurement (see below; Table 1).

	Number of alleles											
	SNPs				Microhomology mediated mutations			Ty insertions				
Gene	**Missense**	**Nonsense**	**Indels**	**Other SNPs**	**MHMI**	**MHMD**	**MHMGC**	**Ty**	**5' Ty**	**3' Ty**	**Other Ty related rearrangement**	**Whole gene deletion**
GAT1	12	2	2	1	1	4	0	47	3	0	0	1
PAR32	1	6	3	0	3	2	0	23	5	0	2	0
MEP1	8	0	0	0	0	0	0	8	0	28	0	0
MEP2	2	0	0	0	0	0	0	0	0	0	0	0
MEP3	2	0	0	0	0	0	0	0	0	0	0	0
FCY2	4	4	2	0	0	1	10	5	1	0	0	0
ARO80	3	0	0	0	0	0	0	1	0	0	0	0
TOR1	1	0	0	0	0	0	0	0	0	0	0	0
TOR2	0	1	0	0	0	0	0	0	0	0	0	0
GPB1	0	0	0	0	0	0	0	1	0	0	0	0
GPB2	2	0	0	0	0	0	0	0	0	0	0	0
SSK2	1	0	0	0	0	0	0	0	0	0	0	0
PDE1	1	0	0	0	0	0	0	0	0	0	0	0

Table 1. Genes with recurrent mutations identified in both haploids and diploids, or whose mutation has been previously shown to be adaptive. Mutations in bolded genes are specifically “nitrogen adaptive” (see below).

Fitness of evolved clones in both limiting nitrogen and glucose

To validate the increased fitness of unique isolated clones that were whole genome sequenced, fitness remeasurements were performed via pooled competitive fitness assay (Methods) in both limiting glucose and limiting nitrogen conditions. This allowed us to distinguish between lineages specifically adaptive in limiting nitrogen, and lineages adaptive in both conditions. The barcoded clones were pooled with 48 confirmed neutral strains from previous experiments (Venkataram et al. 2016), and were competed 1:10 against an unbarcoded ancestor in triplicate. Lineage trajectories were highly reproducible (Figure S1) as were fitnesses calculated from those trajectories (Figure S2).

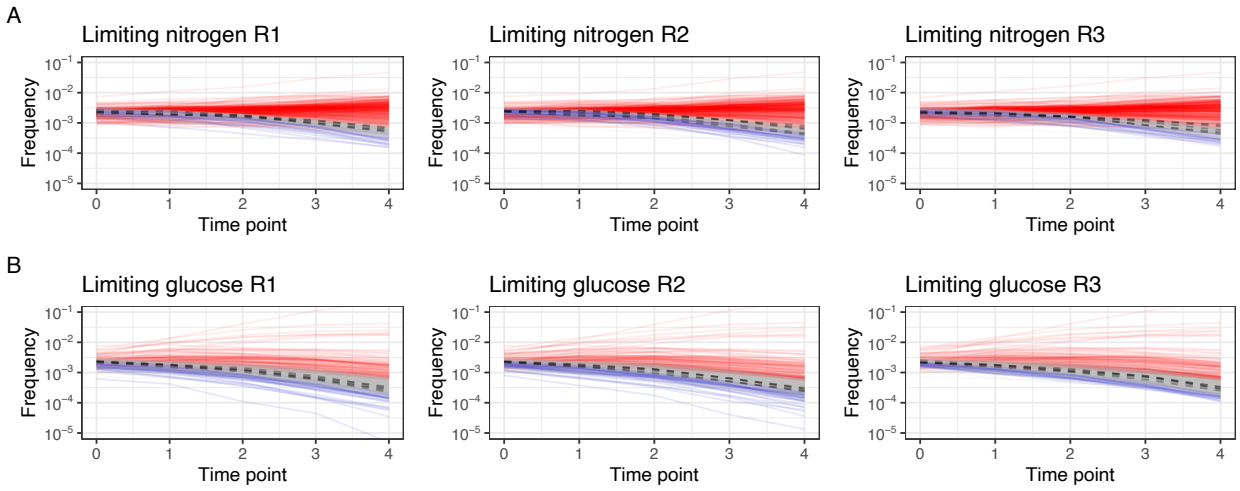

Figure S1. Barcode trajectories during pooled fitness remeasurement experiments, A) in nitrogen limiting conditions, and B) in glucose limiting conditions. A subset of known neutral lineages is represented by dotted lines. Lineages in red have an estimated fitness >0.01, in grey between -0.01 and +0.01, and in blue < -0.01.

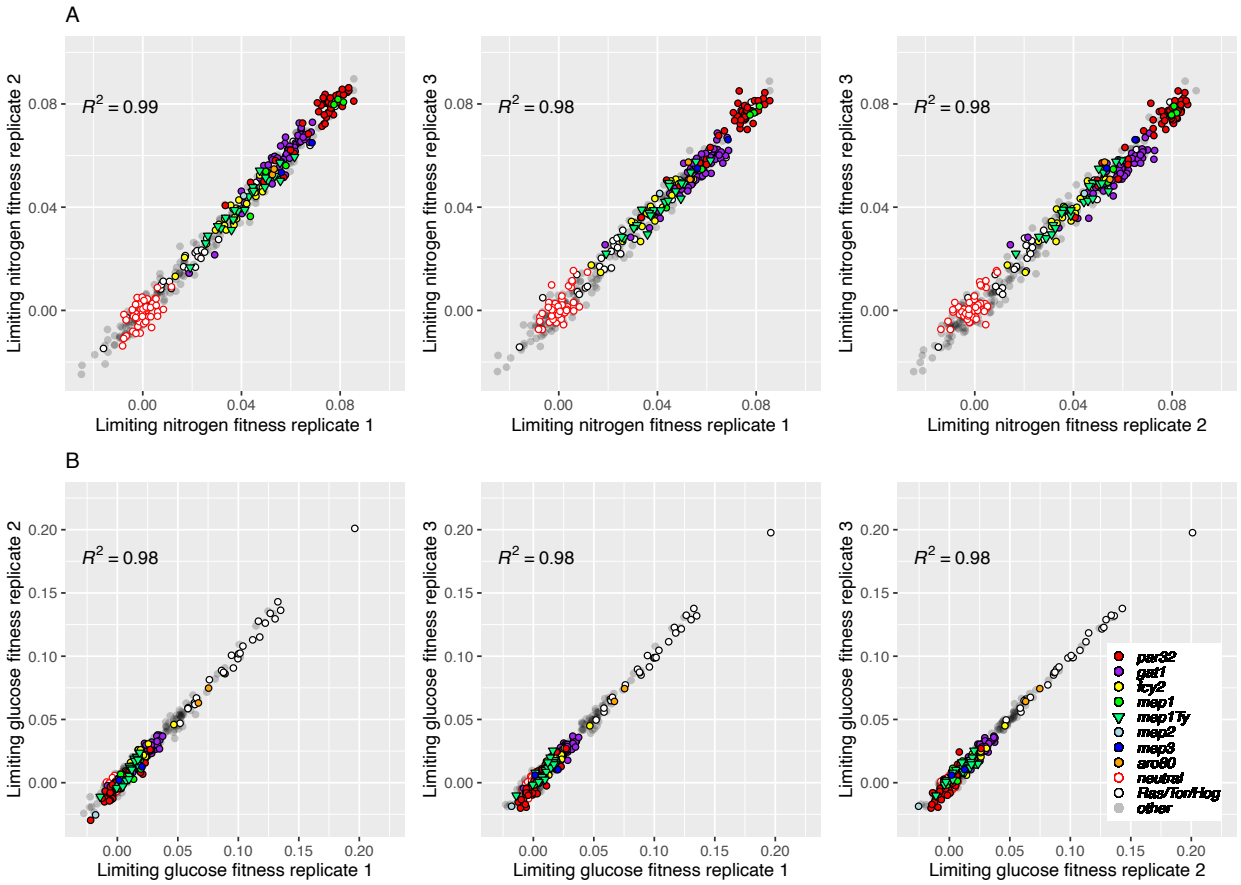

Figure S2. Fitness of isolated clones is reproducible across biological replicates. Estimated fitness between replicates for each clone under A) nitrogen limitation, and B) glucose limitation.

Many of the 332 clones isolated from the nitrogen-limited evolution were beneficial only under nitrogen-limited conditions and were either neutral or even maladaptive in glucose limitation (Figure 1, upper left region), while others were found to be roughly equally beneficial under both glucose limitation and nitrogen limitation (Figure 1, upper right). For the remainder of this manuscript, we focus on genes whose mutation provides substantially greater fitness under nitrogen limitation than under glucose limitation.

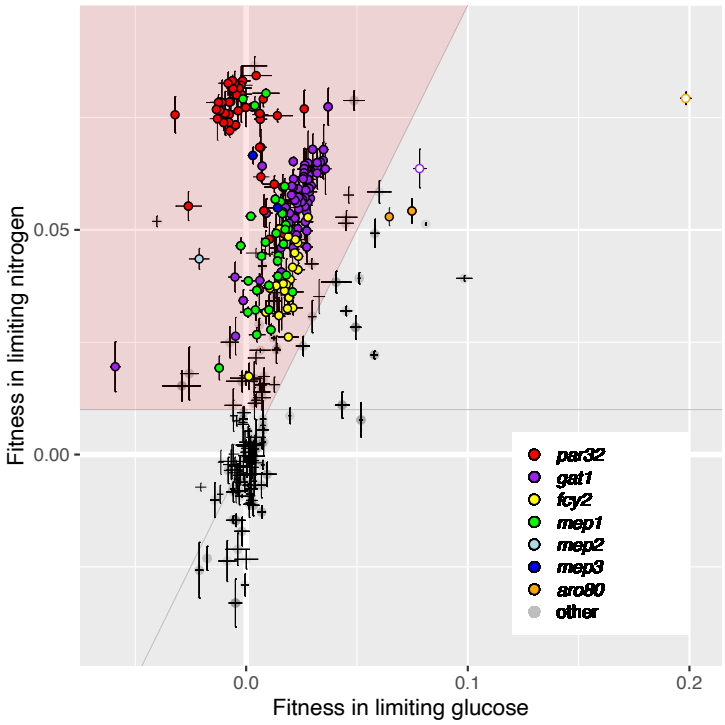

Figure 1. Fitness remeasurements of haploid clones isolated from the nitrogen-limited evolution in nitrogen versus glucose limitation. Clones in the upper left region (pink) are considered to be "nitrogen-adaptive" (see text). The two white-filled circles correspond to double mutants, a *gat1* mutant with a *ssk2* mutation, and an *aro80* mutant with a *gpb2* mutation. Error bars indicate standard deviation of the replicate fitness measurements.

Identification of presumptive beneficial mutations

To classify mutations as specifically adaptive in nitrogen limitation, we identified loci that met three criteria: 1) were recurrently mutated in independent lineages, 2) were also validated to a fitness effect of >0.01 in nitrogen-limited media, and 3) have substantially greater increased fitness in nitrogen limitation than in glucose limitation. Independent lineages were designated by the presence of unique barcodes. We identified six loci that satisfied these criteria, which we refer to as "nitrogen adaptive" from here forward: *GAT1*, *FCY2*, *PAR32*, *MEP1*, *MEP2*, and *MEP3* (Table 1). Together, these loci were independently mutated a total of 193 times across

multiple lineages that exhibited reproducible fitness increases. *MEP2* and *MEP3* were only observed as mutated twice each, with one of the *MEP2* mutations occurring heterozygously in a diploid, while we identified 44 adaptive *MEP1* mutations. Notably, and in contrast to prior results from chemostat evolutions, we did not observe recurrent amplifications at the *MEP* loci: the permeases associated with ammonium import, the limited nitrogen source in this experiment. We identified an additional six loci that had also acquired multiple independent mutations during our evolution; however, they did not show reproducible fitness gains, making the status of these mutations (adaptive or neutral) inconclusive: *MIT1*, *DAL81*, *VID28*, *PFA4*, *CRP1*, and *FAS1*. While *FAS1* was found mutated three times independently in confirmed adaptive lineages, these mutations were only identified in the context of *PAR32* or *GAT1* mutant backgrounds and seemingly did not increase fitness beyond that of the confirmed adaptive alleles. Finally, some loci were mutated and adaptive in both glucose- and nitrogen-limited conditions, including *ARO80* and members of the TOR and RAS pathways: *TOR1*, *TOR2, LST8, SCH9*, and *GPB1* and *GPB2* (Table 1; Supplemental File 1).

Fitness gains and validation of nitrogen adaptive loci

The pooled fitness assays showed that the six recurrently mutated loci consistently correlate with increased fitness in nitrogen limitation, and moreover that different alleles show consistent fitness increases (Figure 1). For example, most of *GAT1* mutations show a reproducible fitness increase of 0.04-0.06/generation, while *MEP1* mutations fall in two clusters with Ty insertions having an average fitness increase of 0.03-0.05 and missense mutations affecting residue Asp262 have a fitness increase of ~0.08. The *MEP2* and *MEP3* alleles showed fitness gains between 0.04 and 0.07. Together, these data show that the evolved alleles at these six loci are indeed adaptive mutations, reproducibly driving 0.03-0.08 increases in fitness in fluctuating nitrogen starvation conditions. To further confirm these mutations are indeed the drivers of fitness gains (rather than ‘hitchhiking’ neutral mutations), we generated progeny for one or more

alleles of each gene for five of the nitrogen adaptive loci and performed a pooled competitive fitness assay as above. The resulting fitness estimates confirmed that the observed fitness gains are correlated with mutations in *GAT1*, *MEP1, MEP2, MEP3, and PAR32*. Progeny show equivalent fitness gains to the adaptive parent, demonstrating that mutations at these loci likely account for all, or nearly all, of the fitness gain in these lineages (Figure 2). Note, the magnitudes of the measured fitnesses are often somewhat smaller than in the fitness remeasurements in Figure 1, we hypothesize that this is a result of the competing pool composition being different (see Methods).

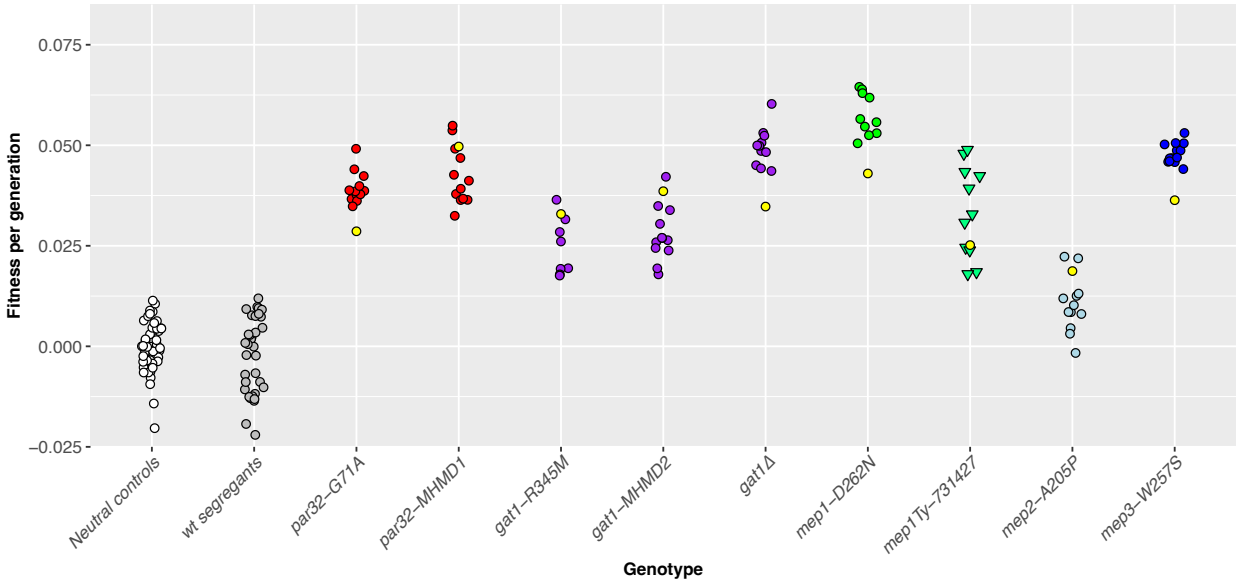

Figure 2. **Fitness remeasurements of progeny containing putatively adaptive alleles confirm adaptive mutations.** Neutral controls are the neutral lineages previously isolated from glucose limited evolutions, while wild-type segregants are segregants from the crosses that lack the adaptive alleles of interest. Yellow dots correspond to the parental lineages.

Targets of adaptation

Lineages with mutations in the six nitrogen-adaptive loci account for 76% of adaptive lineages sequenced in our evolution (178/224 adaptive haploid lineages and 15/29 adaptive

diploid lineages). Here we further discuss the mutation types and allele locations observed and their roles as adaptive targets (Figure 3).

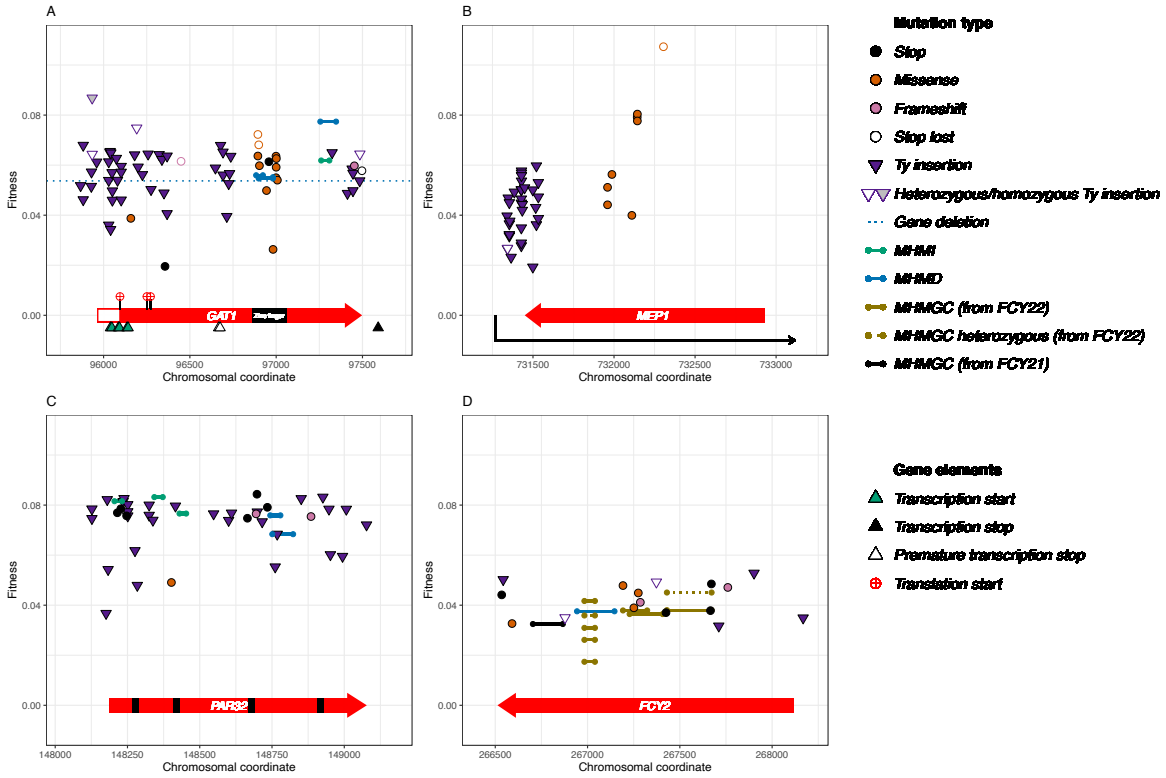

Figure 3. Targets of adaptation and their fitness effects. A) *GAT1*, B) *MEP1*, C) *PAR32*, D) *FCY2*. Glyphs indicate mutation type (see key); the dotted line for *GAT1* indicates the fitness of a complete deletion mutant; the black boxes in *PAR32* indicate repeat regions.

GAT1 locus

GAT1 encodes a GATA-type DNA-binding zinc-finger transcription factor which, among other activities, activates nitrogen catabolite repression (NCR) genes such as *GAP1* and *GLN1*. Gat1 binds DNA directly, but also facilitates transcriptional regulation via protein-protein interactions with other transcription factors (Georis et al. 2009). *GAT1* transcription itself is typically upregulated by Gln3 under nitrogen-limited conditions, reducing nitrogen utilization within the cell. When a preferred nitrogen source is available, Gat1 and Gln3 are phosphorylated by TOR

kinases and are sequestered to the cytoplasm, while *GAT1* transcription is simultaneously repressed by Ure2 and Dal80.

At the *GAT1* locus, novel Ty insertions account for a large proportion (68%) of adaptive mutations (50/73) in this evolution, predominantly inserting in the 5' half of the CDS (Figure 3A). However, other classes of mutations were also observed in *GAT1*, including two nonsense mutations, two frameshift mutations, a lost stop codon, several short, out-of-frame intragenic rearrangements that likely arose by microhomology mediated recombination (Figure 3A and Figure 4B), and 12 missense mutations, as well as a whole-locus deletion (3.9 kb, from 722bp upstream to 1.6kb downstream).

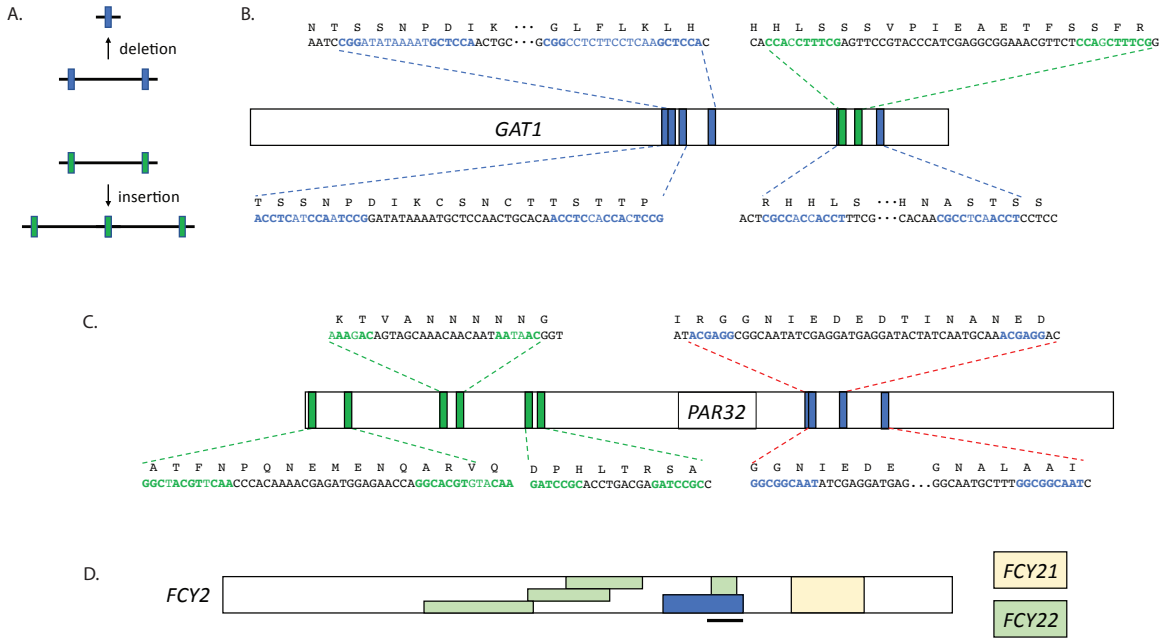

Figure 4. Microhomology-mediated mutations. A) diagram of how sequence flanked by regions of microhomology can either be deleted or duplicated; color is used to denote insertion vs. deletion. B) microhomology mediated mutations in *GAT1*, C) microhomology mediated mutations in *PAR32*, and D) regions of *FCY2* replaced by ectopic recombination from either

FCY21 or *FCY22*; one of the *FCY22* gene conversions was observed five independent times. The blue box in *FCY2* indicates the location of a microhomology mediated deletion, while the black bar indicates the location of previously observed gene conversion events in *FCY2* (Quinto-Alemany et al. 2012).

Several (8/29) adaptive diploid clones were isolated bearing *GAT1* mutations (open shapes, Figure 3A) in addition to the 65 haploids. Diploidization alone gives rise to increased fitness of ~0.03, while diploids with heterozygous missense mutations at *GAT1* experience fitness increases of 0.06-0.07, similar to *GAT1* mutant haploids. Homozygous *GAT1* mutants had even larger fitness gains. For example, a single diploid with a homozygous *GAT1* mutation (Ty insertion, putative null, also observed in a haploid background) was identified for which we measured a fitness increase of greater than 0.08. Additionally, several of these adaptive mutations putatively affect the *GAT1* RNA isoforms differentially (triangles below gene name), either through impacting alternate start (green triangle) or alternate stop sites (yellow and red triangles). Across both haploid and diploid clones, all but one (11/12) of the missense mutations affecting *GAT1* (Figure 3A, burgundy circles) fall within the zinc-finger domain and show fitness increases of ~0.06, similar to the putative null mutant alleles. We also identified two alleles with small deletions in the zinc finger domain that each result in a frameshift that truncates Gat1.

In our study, we observe adaptive *GAT1* alleles with polymorphisms at the DNA-binding site, as well as putative null mutations. These adaptive alleles all show similar fitness increases (0.06±0.01) in haploid isolates. Given the many mechanisms by which Gat1 affect NCR regulation, these alleles may act on cell fitness through similar or differing mechanisms: Gat1 DNA binding mutants maybe functionally null, explaining the similarity in fitness increase, or perhaps DNA-binding mutants impact fitness through alternative means, such as modulating Gat1p protein-protein interactions with other transcription factors.

The NCR program allows cells to increase their uptake and usage of non-preferred nitrogen sources during low nitrogen abundance but is repressed in the presence of preferred nitrogen sources. *GAT1* null mutations may be beneficial under these evolution conditions (serial transfer in ammonium-limited media) as *gat1* cells may be better poised to immediately utilize the nitrogen available upon transfer to new media, relative to *GAT1* competitors that would require repression of NCR factors to utilize the freshly-introduced nitrogen supply. For this reason, *gat1* null alleles may be most likely to be beneficial in cells experiencing fluctuating ammonium concentrations from moderate (3 mM) to total nitrogen starvation. While *GAT1* alleles have also been shown to be beneficial in constant low nitrogen chemostat environments (Hong et al. 2018; Abdul-Rahman et al. 2021), only adaptive DNA-binding SNP mutations were identified in that study. No null alleles were observed in adaptive clones or populations evolved in chemostat low ammonium conditions, even in ultradeep targeted sequencing experiments (Hong and Gresham 2014). When *gat1* null allele fitness was assessed in those conditions they did not observe increased fitness (Hong et al. 2018).

MEP loci

S. cerevisiae has three paralogs, *MEP1, MEP2, and MEP3,* that encode permeases for ammonium, the nitrogen source used in this study; these transporters have differing affinities for ammonium and are induced at different levels in response to the quality and quantity of the nitrogen source (Marini et al. 1997). Mep1 forms a heterotrimeric complex with Mep3, while Mep2 forms a homotrimeric complex (see Boeckstaens et al. 2015). The Mep1/3 complex is inactivated by Par32 binding (Boeckstaens et al. 2015; see below), while Mep2 is regulated directly via Npr1 phosphorylation (Boeckstaens et al. 2007). In our evolution conditions, we observe 44 independent mutations affecting the *MEP1* locus, and just two mutations each at *MEP2* and *MEP3* loci (Figure 3B; Table 1, Figure S3). Fitness effects of the *MEP2* and *MEP3*

mutations were comparable to some missense *MEP1* mutants (~0.04-0.06), while the fittest *MEP1* mutants conferred up to 0.08 advantage in haploids.

Notably, we found no evidence for amplification of the *MEP* transporters in adaptive clones, only the missense and Ty derived alleles described here. This is in contrast to the amplification of genes encoding relevant permeases observed under constant nitrogen limitation in chemostats (Hong and Gresham 2014; Gresham and Hong 2015). This observation supports that how selection is applied (e.g. fluctuating vs. constant) under nitrogen limitation changes the spectrum of adaptive mutations recovered, as was observed under glucose limitation.

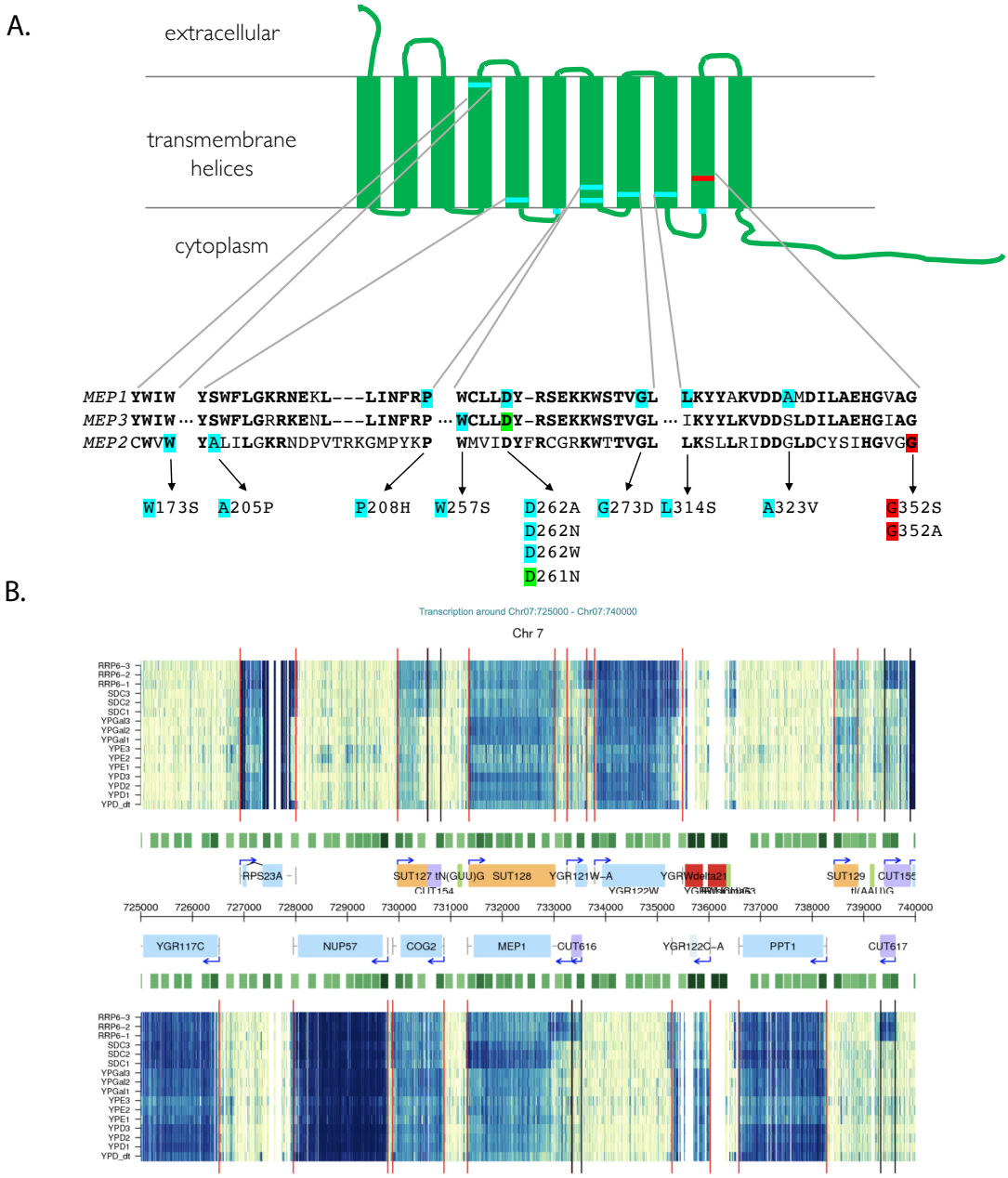

Figure S3. Locations of *MEP* mutations and antisense transcript at the *MEP1* locus. A) Locations of Mep mutations in a multiple alignment; the green highlighted residue identifies which gene had that mutation, while the red highlighted residues were mutations observed

previously (Hong and Gresham 2014), and B) transcription at *MEP1* locus indicates the presence of an antisense transcript downstream of *MEP1*.

We observed four independent missense mutations that affected Asp261/262 in *MEP3* and *MEP1*, respectively. Strikingly, two of these resulted in an identical substitution in *MEP1* and *MEP3*, from Asp to Asn (Figure S3A). Others have observed *MEP* mutations under nitrogen-limited chemostat evolution conditions, interestingly only in *MEP2*, not in *MEP1/3* (Hong and Gresham 2014). It is possible that the missense mutations at these sites give rise to a higher affinity ammonium transporter in all cases, but that differences in constant vs. fluctuating nitrogen-limited environments determine which transporter is most important or active.

In addition to missense mutations, we observed a striking pattern of Ty insertions at the *MEP1* locus (Figure 3B), with 36 novel insertions falling in the 3' UTR and the 3' most region of the gene. These insertions fall close to the 5' end of an antisense transcript (SUT128) that has been observed in RNA-Seq experiments (Xu et al. 2009; Figure S3B). The group of Ty insertions in the 3' region unique to the *MEP1* locus may affect fitness in nitrogen limitation via a mechanism different than the putative gain of function missense mutations in the coding region itself. These alleles may be increasing Mep1p activity (via RNA regulation for example) or affecting NCR regulation independently of Mep1p. *MEP1* expression is normally controlled by nitrogen catabolite repression regulation via TORC1p and Par32p (Boeckstaens et al. 2015). The lack of such insertions downstream of either *MEP2* or *MEP3* suggest that this mode of regulation may be unique to *MEP1*.

Because serial transfer in ammonium-limited conditions gave rise to two main classes of adaptive mutation in *MEP1* (missense mutations in the transport domain, and 3' Ty insertions) and similar missense mutations in *MEP2* were observed in chemostat ammonium-limited

conditions, we asked whether continuous culture conditions also give rise to Ty insertions near *MEP* genes. We reanalyzed the data from (Hong and Gresham 2014) (see Methods) to look for Ty insertions at *MEP1/2/3* and found no evidence for adaptive Ty insertions at these loci. This suggests that 1) Ty elements are less active under continuous culture conditions (even when the same nutrient is limiting), or 2) that the mechanism by which Ty insertions are beneficial under fluctuating nitrogen starvation conditions is not equally adaptive in constant low-nitrogen conditions, or 3) a combination of both. We speculate that the adaptive *MEP1* missense alleles observed in our study may in fact be gain of function mutants, capable of transporting ammonium more effectively, while the downstream Ty insertions may increase Mep1 activity through other means.

PAR32 locus

We observed 45 independent beneficial *PAR32* mutations, predominantly comprised of putative null alleles [44/45], including nonsense mutations, Ty insertions or frameshift mutations (Figure 3C), and just a single adaptive missense allele. Five frameshift alleles all likely arose by microhomology-mediated recombination (Figure 4C). Most of the putative null alleles are associated with a ~0.08 fitness increase, suggesting that lack of Par32 gives rise to similar host fitness benefits regardless of mutation type that creates the null allele. Par32 is an unstructured protein known to inhibit Mep1/Mep3 transporters, so *par32* null alleles likely affect fitness through increasing Mep activity, just as *MEP* loci gain of function alleles would be beneficial in these same evolution conditions (Boeckstaens et al. 2015). Consistent with this, the *par32* alleles fitness effect is similar to the effect of the fittest *mep1* alleles (~0.08). We observed only one *PAR32* missense mutation (Figure 3C, burgundy circle). This missense mutation lands in the second of four repeat motifs (Figure 3C, black bars) found in Par32; these repeat regions are essential for direct Par32 interaction with the Mep proteins (Boeckstaens et al. 2015).

Null *par32* alleles are likely to be adaptive by preventing the inactivation of Mep1/3 transporters specifically during fluctuating low-to-no nitrogen conditions. *par32* null alleles may facilitate more rapid uptake of nitrogen when moved to fresh medium containing ammonium relative to wild type cells that would need to re-activate Mep1/3 expression. Under continuous culture conditions where low ammonium concentrations remain steady and do not drop to zero, others have observed that *par32* null mutants are actually maladaptive (Abdul-Rahman et al. 2021).

FCY2 locus

Finally, we found the *FCY2* locus mutated in 27 lineages in our evolution (Figure 3D). *FCY2* is a purine-cytosine permease found at the plasma membrane, important for the import of adenine and other substrates into the cell (Hopkins et al. 1992; Ferreira et al. 1997; Ferreira et al. 1999; Kurtz et al. 1999; Wagner et al. 2001). Ten out of the 27 *FCY2* beneficial mutations are microhomology-mediated gene conversions with regions of other *FCY* genes (*FCY21* and *FYC22*; Figure 4D) resulting in frameshifts. Fcy21 and 22 are both nucleobase transmembrane transporters, but cannot functionally replace Fcy2 (Wagner et al. 2001). Such gene conversion events have been observed previously between *FCY2* and *FCY22*, but not involving *FCY21* (Quinto-Alemany et al. 2012). These regions of gene conversion likely decrease or abrogate the transport function of Fcy2 as was seen previously (Quinto-Alemany et al. 2012). The *FCY21/22* converted alleles show average fitness increases of ~0.04.

Additionally, we observed several Ty insertions in the 5' region of the CDS of *FCY2* (Figure 3D, Table 1) as well as both nonsense and frameshift mutations, suggesting that null alleles are also beneficial under nitrogen starvation. These mutations exhibit a similar range of fitness increases, again suggesting that a decrease in *FCY2* activity is likely adaptive in ammonium-limited serial transfer.

Timing and establishment of adaptive mutations

Through barcode lineage tracking and comparison to neutral fitness lineages, we explored the relative dynamics of adaptive allele establishment in the population (Figure S4). We note that the lower fitness, but still adaptive, alleles (such as mutations of *fcy2,* yellow Figure S4 panel E) established early in the evolution, while single mutations corresponding to larger fitness increases (e.g. *PAR32* and *GAT1*, red (panel A) and purple (panel B) respectively) increased more rapidly but arose later in the evolution. These observations may reflect the 'ease' of acquiring these mutations: for example, *fcy2* appears to be the result of a gene conversion event, which may arise more often than inactivating point mutations in *par32 and gat1*, or the putative gain of function mutants in *MEP* genes. In addition to how frequently some mutation types occur, the relative fitness of a mutation shapes how quickly those adaptive lineages expand in the population. As we have observed previously (Levy et al. 2015), lower fitness adaptive mutations arise early during evolution, while higher fitness single mutations can occur later and still reach population frequencies high enough to be sampled in our clonal sequencing (Figure S4 panel F).

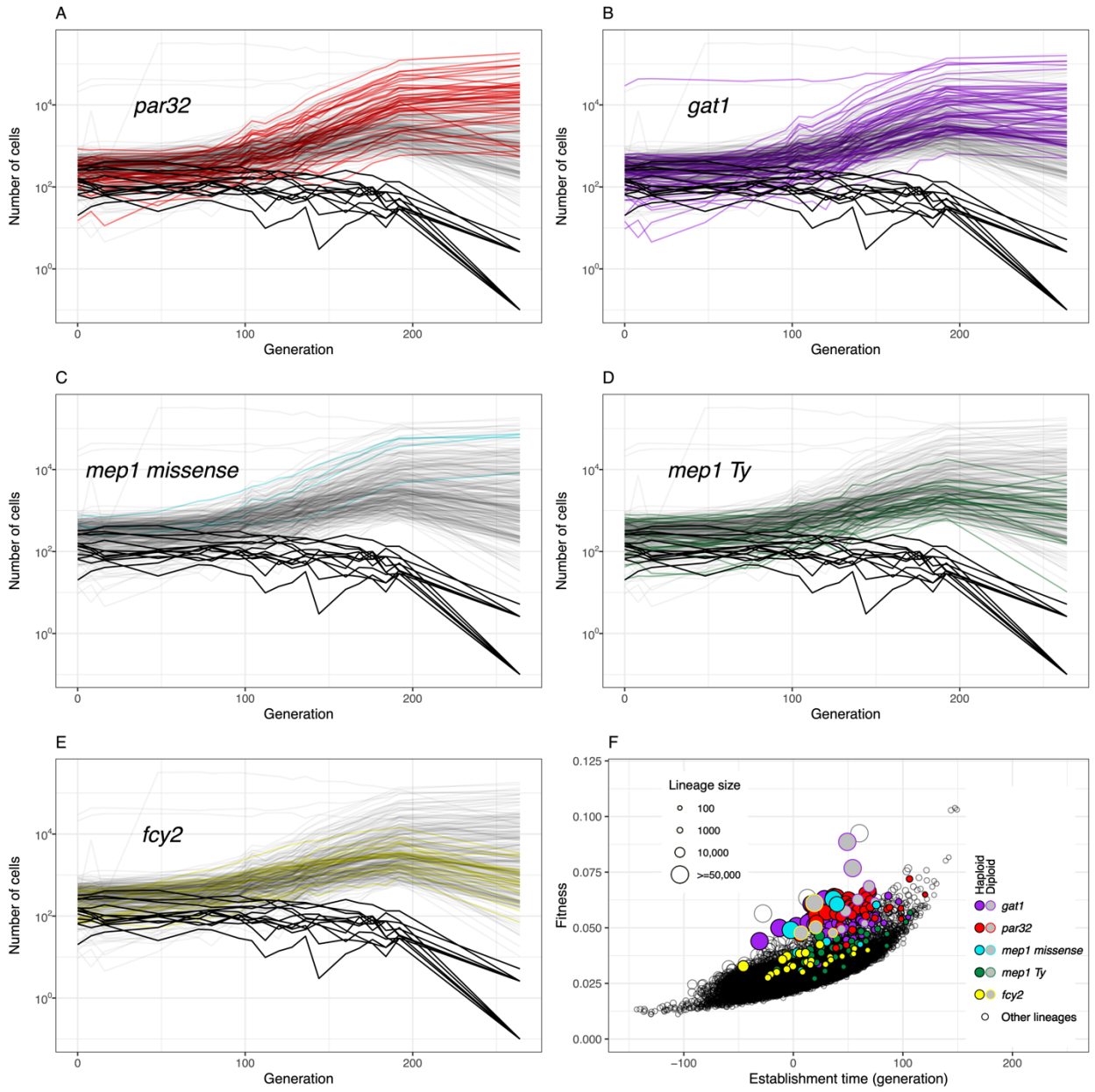

Figure S4. Dynamics of increase in frequency of lineages with adaptive mutations in specific genes. A) *PAR32* (red), B) *GAT1* (purple), C) *MEP1* missense mutations (light blue and burgundy), D) *MEP1* Ty insertions (green), E) *FCY2* (yellow), and F) fitness and lineage size as a function of establishment time (color-coded the same way as panels A-E).

Mutational spectra in nitrogen- vs. glucose-limited populations: Increased Ty transposition in nitrogen-limited conditions

To better understand the classes of adaptive mutations underlying genome evolution, we compared the mutational spectra observed in both neutral and adaptive populations under both nitrogen and glucose limitation. First, we note that autodiploidy itself confers a significant fitness benefit in both nitrogen limitation (Blundell et al. 2019) and glucose limitation (Venkataram et al. 2016). Beyond autodiploidy, we observed that in both neutral and adaptive haploids, SNPs comprise the majority of genome changes under glucose limitation (Figure 5A) and in both glucose and nitrogen-limited conditions SNPs were enriched in adaptive lineages relative to neutral lineages (black bars, Figure 5A). By contrast, in our haploid clones, Ty insertions are most prevalent under nitrogen limitation, with approximately ~2.6 novel insertions per clone compared to only ~0.47 novel Ty insertions in haploid clones from glucose-limited evolutions (Figure 5A). Novel Ty insertions were more prevalent in neutral than adaptive lineages (blue bars), however in nitrogen limitation in particular, Ty mutagenesis accounts for a substantial number of adaptive mutations (gold bar). In 345 nitrogen evolved clones (including both haploid and diploid isolates) we observed 898 novel Ty insertions, while we found only 212 novel Ty insertions in 488 glucose evolved clones (Figure 5B).

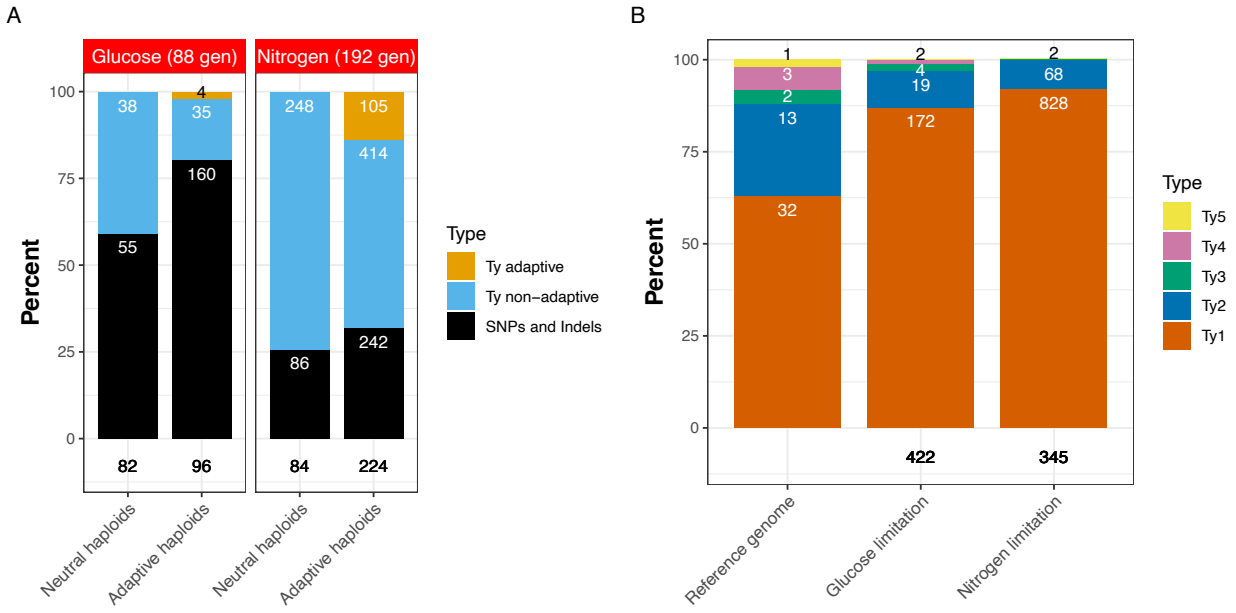

Figure 5. Ty activity is increased in fluctuating nitrogen-limited conditions and gives rise to a significant number of adaptive alleles (A) Observed mutational types in neutral and adaptive haploid clones isolated under glucose and nitrogen limitation. (B) Ty activity in both haploids and diploids evolved under nitrogen and glucose-limited conditions relative to the ancestral strain (reference genome). Stacked bar charts represent the fraction of each Ty type (Ty1-Ty5) present in the reference genome, or of novel insertions identified in clones evolved in the nitrogen- and glucose-limited conditions. Numbers on bars represent raw counts of the given Ty type. Numbers below the stacked bars indicate the number of strains from which the novel insertions were observed.

Not all Ty families are equally activated under nitrogen limitation

To better understand how nitrogen limitation increases transposition, we examined which Ty elements in the ancestral strain were most active under these conditions as compared to under glucose limitation (Figure 5B). Others have observed Ty1 and Ty2 to be the most active classes of spontaneous Ty transposition (Curcio et al. 1990), and the novel insertions observed in both our glucose- and nitrogen-limited evolved strains reflect that (Figure 5B). Ty1 is the most prevalent class in the ancestral strain (accounting for 32/50 intact Ty insertions). In nitrogen limitation, Ty1 accounts for 92% (828/898) of novel insertions with Ty2 accounting for just the remaining 8% (68/898), as opposed to the 26% of insertions in the ancestor. Ty1 is also frequently the most activated Ty element in *S. cerevisiae* under other stress conditions (Morillon et al. 2000; Morillon et al. 2002). In glucose-limited clones, Ty1 accounts for 87% of novel insertions (172/197), while Ty2 accounts for ~10% (19/197) of novel insertions. In the ancestor, Ty3 and Ty4 account for 4% and 6% of insertions respectively, but just 0.2% (2/898) of Ty3 in nitrogen-limited clones. The single copy of Ty5 in the ancestor is known to be inactive and gives rise to no new insertions under either glucose or nitrogen limitation. The distributions of novel Ty insertions by Ty types are significantly different in nitrogen- and glucose-limited evolved clones

compared to the distribution of Ty insertions in the reference genome (chi-squared p-value = 1.3e-71 and 1.4e-10, respectively), suggesting, as has been seen previously, that not all Tys or Ty classes are equally active. The distributions of Ty classes in the set of novel insertions those clones evolved in nitrogen and glucose also differ significantly (p=3.4e6).

Taken together these data suggest that while Ty activity is substantially increased under fluctuating nitrogen conditions (as compared to both glucose limitation and constant nitrogen limitation), that not all Tys are equallt activated, with Ty1 and Ty2 being the predominant *de novo* insertions. It remains to be investigated whether this activity is due to increased transcription or reinsertion, or if there are differences in Ty subclass activity, or specific Ty insertions giving rise to the novel insertions.

Adaptive Ty insertions enriched in ORF regions

Ty elements preferentially target gene-poor regions and Ty1 in particular has been observed to most often land upstream of genes transcribed by RNA polymerase III, such as tRNA and snRNA genes (Devine and Boeke 1996). In the hundreds of such Ty insertions that arose in nitrogen and glucose limitation we observed a periodicity of their insertion locations (Figure S5) suggesting not only tRNA proximity bias, but also preference for nucleosome free regions, consistent with previous observations (Mularoni et al. 2012). A larger proportion of mutations in nitrogen neutral haploids were due to Ty element insertions (74%) relative to in adaptive mutants (68%) (Figure 5A); however, the locations of adaptive Ty insertions show striking clusters at some of the nitrogen-adaptive loci (Figures 3 and 5), sites not typically preferred by Ty1.

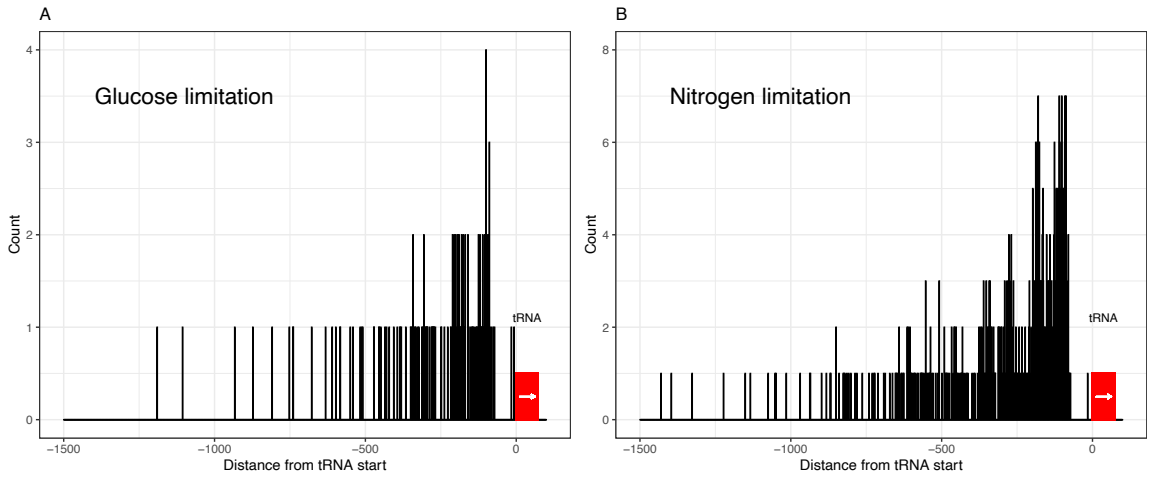

Figure S5. Insertion locations of Ty elements upstream of tRNA genes in A) glucose limitation and B) nitrogen limitation

Discussion

Here we profiled adaptive mutations that arose in nitrogen-limited yeast cultures under conditions fluctuating between low-nitrogen and total nitrogen starvation (Blundell et al. 2019). We observed that frequent Ty transposition and microhomology-mediated recombination events are responsible for a large number of adaptive mutations. This is in contrast to glucose limitation under similarly fluctuating conditions, where self-diploidization and SNPs/short indels gave rise to most adaptive lineages (Levy et al. 2015; Venkataram et al. 2016). Adaptive clones that arise to high frequency early in the evolution under glucose limitation show larger fitness effects than the respective clones under nitrogen limitation, accounting for the difference in the population dynamics (Blundell et al. 2019). Whether this reflects the altered spectrum of mutational types, or is simply a result in the difference of strength of selection and distance from the fitness optimum is unclear, though these possibilities are not mutually exclusive.

In contrast to our observations in serial transfer experiments under nitrogen limitation, increased Ty activity is not a frequent mechanism of adaptation under nitrogen-limited continuous culture conditions, where cells experience a nutrient poor condition but never experience total starvation (Gresham et al. 2010; Gresham and Hong 2015). Instead, copy number variation of nitrogen transporters most often drives adaptation under continuous low nitrogen (Gresham et al. 2010). This adaptive mechanism bears resemblance to the means of adaptation observed in glucose-limited chemostats, where the copy number of *HXT* hexose transporters is often amplified, facilitating increased glucose uptake (Brown et al. 1998; Gresham et al. 2008; Kao and Sherlock 2008). This suggests that despite different metabolite restrictions, chemostat evolution predominantly favors adaptation via increased abundance of transporters for the limiting nutrient, indicating these mutations arise most often and/or are the most fit. Similarly, in chemostat sulfate limitation amplification of *SUL* transporters is observed to be the most common adaptation (Gresham et al. 2008; Payen et al. 2014; Sanchez et al. 2017). Taken together these results suggest that an adaptive 'winning strategy' under chemostat conditions favors increases in transporter abundance, regardless of the specific nutrient restriction. While these amplifications are not the sole means of adaptation, the prevalence of these amplifications reflects both how easy these changes are to achieve (relative frequency of mutation type) and how beneficial (degree of fitness increase) these changes are specifically in the low, but not zero, nutrient availability conditions of a chemostat. This suggests that under fluctuating conditions the period during the growth cycle in which additional transporters might be beneficial is insufficient to drive them to high frequency under such conditions – indeed, such amplifications may be deleterious at the beginning of a growth cycle, when the medium is replete with the eventually limiting nutrient (Wenger et al. 2011).

Under serial transfer conditions, nutrient availability fluctuates and cells may even experience total starvation for the limiting nutrient. Previous work from our lab and others shows that under

fluctuating glucose limitation self-diploidization and SNPs affecting the TOR and Ras pathways arise to high frequency early during such evolutions (Venkataram et al. 2016). These mutations improve fermentation performance and also drive adaptation through decreasing time in lag phase upon reintroduction of fresh glucose (Li et al. 2018). By contrast, here we find that Ty and microhomology-facilitated mutations contribute substantially (though not exclusively) to the suite of adaptive mutations observed under nitrogen-limited serial transfer. This suggests two things: first, unlike chemostats, where the common 'strategy' for adaptation is frequently transporter copy number amplification, serial transfer does not initially favor a specific class of genomic changes irrespectively of the restrictive nutrient. Second, stably nitrogen poor conditions give rise to different adaptive 'routes' than fluctuating conditions where cells experience total nitrogen starvation. This may be due, at least in part, to some mutagenic mechanisms, such as transposon activity, being more or less active under nitrogen poor vs. starving conditions.

The significant increase of Ty activity under this specific fluctuating nitrogen-starvation condition, relative to glucose limitation and chemostat conditions, raises the question as to what drives this increase, specifically in Ty1 activity. Ty1 derepression could be associated with host cell transcription changes due to stress, accumulation of other mutations (Staleva Staleva and Venkov 2001) or even disruption of the Ty elements themselves, some of which restrict other subclasses of Ty (Czaja et al. 2020). Ty1 is known to contain a self-limiting restriction factor (p22) that facilitates copy number control within the host cell; it will be interesting to further explore how host nutrient starvation sensing interacts with this restriction pathway (Nishida et al. 2015; Saha et al. 2015; Tucker et al. 2015; Ahn et al. 2017).

The increase in novel Ty insertions could also be due to increases in Ty reinsertion, or frequency of Ty reimport into the nucleus, rather than transcriptional activation. Studies determining at which step(s) of the Ty life cycle nitrogen starvation shapes ty activity would be

needed to determine the specific mechanism underlying the increase in transposon insertions. Others have shown that Ty1 activity is sometimes due to an increase in transcription at specific Ty1 loci, during both severe adenine starvation and when environmental conditions trigger the invasive growth pathways - which includes nitrogen starvation (Company et al. 1988; Laloux et al. 1990; Laloux et al. 1994; Conte et al. 1998; Morillon et al. 2000; Morillon et al. 2002; Lesage and Todeschini 2005; Sacerdot et al. 2005; Todeschini et al. 2005; Rutherford et al. 2008; Servant et al. 2008; Servant et al. 2012). It has also been shown that this transcriptional increase is not equal amongst Ty elements, and that specific transposons were activated more than others. If the observed increase in novel Ty insertions in our results is also due to an increase in Ty transcription from a specific subset of originating loci (possibly the same subset as in (Morillon et al. 2002) it will be interesting to understand the mechanism underlying this insertion-specific activation.

The observed repertoire of beneficial mutations reflects both the underlying rate at which such mutations arise, as well as their resulting fitness. As such, we find it notable that some mutational mechanisms appear to be differentially active under certain environmental conditions, as is the case with Ty activity under fluctuating nitrogen starvation. This association of environmental stress with increase in Ty activity could also be a mechanism for stress induced mutagenesis (Galhardo et al. 2007; Ram and Hadany 2014). If cells experience increased mutation rates while under stress conditions, but not under regular growth conditions, this could improve the overall population's chances of survival. Host populations would sample greater genetic and phenotypic variation while experiencing conditions they might not otherwise survive, without the mutational burden during times of high fitness. A Ty insertion that is primarily silenced, but then active during extreme nutrient starvation could provide additional host adaptive potential. Indeed, if global Ty derepression reflects a host-parasite coevolution that minimizes host cost and maximizes potential for survival of both, the role of transposons in

host evolvability is important (Levin and Moran 2011). If some strains are poised to “turn on” mutagenesis under otherwise deadly stress conditions, selection could favor these backgrounds; further evolutionary analysis of Ty insertions associated with starvation-induced activity could reveal one facet of selection shaping host-transposon coevolution (Bleykasten-Grosshans et al. 2021).

Alternatively, rather than being beneficial under stress and the trait being selected for, Ty activity may not have been strongly selected against in starvation conditions, or may be impacted by historical survivor bias. Although competent under lab conditions, Ty elements rarely “hop” (Scholes et al. 2001), so perhaps the correlation of Ty activity to stress response and environmental fluctuations is somewhat analogous to the meiosis-linked transposable element hopping in metazoans, where it is thought to minimize somatic damage and maximize spread in sexual populations (Haig 2016). Maybe low Ty activity was selected for during favorable yeast growth conditions, and the relative increase in activity reflects a lack of historical negative selection under nitrogen starvation. If this is the case, it would be interesting to better understand the mechanistic basis of why increased Ty mobilization occurs in total nitrogen starvation but not under constant low nitrogen conditions. Exploring the activity of transposons in other yeast species, including those with different lifestyles, such as pathogens, could provide further insight into the complex relationship between host and transposon coevolution (Maxwell 2020).

While Ty activity was notably increased under the evolution conditions we studied here, there were several other mutational mechanisms that were active and gave rise to multiple adaptive mutations. Notably, microhomology-mediated changes gave rise to gene conversion, duplication and deletion events. There are several mechanisms that can result in structural changes at sites of microhomology, including recombination and end-joining mechanisms, but also DNA

replication-based mechanisms, such as fork stalling and template switching, or microhomology-mediated break-induced replication (Ottaviani et al. 2014). Like Ty activation, these mechanisms may occur more frequently than point mutations in the genome, and because of homologous sequences, can impact some regions of the genome more frequently than others. Homology-rich regions could be regions of instability relative to other parts of the genome, shaping host evolvability at those sites in particular, and potentially minimizing deleterious effects elsewhere in the genome.

Several of the adaptive alleles we identified would likely have been missed in a classic loss-of-function genetic screen, including Ty and microhomology alleles, but also some SNPs, such as the putative gain-of-function missense mutations in the *MEP* genes. In other cases, we identified adaptive alleles that we predict are null mutants, and that would be (and in some cases have been) identified in genetic screens. By taking an experimental evolution approach we also learn about the competitive fitness of these alleles – information that is not generated in most genetic screens. This emphasizes both the utility of experimental evolution for understanding the genetics of phenotypes of interest, but also how complementary this approach is to classical genetics.

When exploring a trait of interest, experimental evolution can both expand upon and reinforce lessons learned through other approaches. Natural variation in extant strains and species can help clarify what *has* happened in naturally evolving populations, but the context of those changes and their fitness consequences may not always be clear. Experimental evolution can leverage large populations and controlled selective pressure to understand how genomes *can* evolve, what mechanisms give rise to novel alleles, and the relative fitness of those alleles. The alleles sampled will be shaped by the likelihood of their occurrence: the frequency is driven by the mutation mechanisms active in those cells, which can be shaped by the cells' environment,

and the ‘best’ alleles will be those that provide the biggest fitness gains under the specific selective pressure. Lower fitness adaptive mutations can be well represented particularly if they arise more readily (such as autodiploids), or if they occur early in an evolution and secondary adaptive mutations are then also acquired. Often in genetic analyses, emphasis is placed on coding SNPs. While this class of mutation undeniably shapes how genomes evolve and organisms adapt, there are many other mutational mechanisms driving biological innovation. Studying the full complement of mutational mechanisms, and the spectrum of alleles that they create, provides a deeper understanding of important biological processes.

Methods

Isolation and sequencing of evolved clones

Isolation of clones analyzed in this work were described previously (Venkataram et al. 2016; Blundell et al. 2019). Briefly, we isolated evolved clones from nitrogen- and glucose-limited evolutions from generation 192 and generation 88, respectively (Venkataram et al. 2016; Blundell et al. 2019). Frozen aliquots from the appropriate time point were suspended in water and plated on SD-Ura plates. Single colonies were picked in unbiased fashion, suspended in 15 µl of water, and aliquots were saved for barcode PCR, ploidy determination (using a medium throughput benomyl sensitivity test (Venkataram et al. 2016)), and for storage in 25% glycerol at -80°C. Haploid clones from independent lineages with fitness (as estimated from barcode trajectories during the nitrogen-limited evolution experiment) over 0 and self-diploidized isolates with fitness over 0.03, as well as 12 neutral clones were whole genome sequenced as described (Blundell et al. 2019).

Fitness remeasurement experiments

The 345 sequenced clones isolated from the nitrogen-limited evolution were pooled with 48 strains that were designated as having neutral fitness based on previous experiments (Venkataram et al. 2016). The barcoded pool was then mixed with 90% unbarcoded wild-type (to minimize the change in population mean fitness during the experiment) and propagated via serial transfer for four transfers in either glucose-limited or nitrogen-limited media (as previously (Levy et al. 2015; Blundell et al. 2019)). Barcodes were sequenced at each transfer, and fitness of clones was estimated from their barcode frequencies as described (Blundell et al. 2019).

Multiplexed barcode sequencing

To determine individual barcodes in the selected clones, 5μL of the suspension was lysed in 30μL of lysis buffer (1mg/mL Lyticase (Sigma L4025-250KU), 0.45% Tween20, 0.45% Igepal CA-630, 50mM KCl, 10mM Tris-HCl pH 8.3 (adapted from (Kwiatkowski et al. 1990)). 2.5μL of lysed cells were amplified in a 25μL PCR reaction with 12.5μL of 2xOneTaq mix, 5μM of Forward (F(n)) and Reverse (R(n)) multiplexing primers (Table S1) and water as follows: 94°C x 2', 35 cycles of 94°C x 30", 48°C x 30", 68°C x 30".

52 plates of clones were multiplexed and barcodes were sequenced in two paired-end 300bp MiSeq runs.

Whole genome sequencing.

DNA for whole genome sequencing was prepared using YeaStar Genomic DNA kit (ZymoResearch D2002). Sequencing libraries were prepared using the Nextera kit (Illumina FC-121-1031 and FC-121-1012) as described in (Kryazhimskiy et al. 2014), starting with 5-10 ng of genomic DNA. Resulting libraries from each 96-well plate were pooled at an equal volume. Pooled libraries were analyzed on the Qubit and Bioanalyzer platforms and sequenced paired-end 100bp on HiSeq 2000 (one lane per 96 clone pool).

Variant and Ty insertion calling using CLC Genomics Workbench 11

Short reads from whole genome sequencing were trimmed to remove the adapter sequence and mapped (match score 1, mismatch cost 2, Linear gap cost: insertion 3, deletion 3, length fraction 0.5, similarity fraction 0.8) to *S. cerevisiae* reference genome (R64-2-1_20150113). SNPs and indels were called ignoring broken pairs with 85% minimal frequency in haploids and 35% minimal frequency in diploid strains, with base quality filter 5/20/15, direction frequency filter 5% and significance 1%, and read position filter 1%. Structural variation was called using InDels and Structural Variants identifying novel breakpoints. Breakpoints output from the InDels and Structural Variants calling (using the default settings) were used to identify Ty insertions (maximum 15% mapped perfectly for haploids and maximum 70% mapped perfectly for diploids). Breaks were filtered for unaligned sequences specific for LTRs and verified visually in the CLC Genomics Workbench browser.

Identification of Ty insertions using RelocaTE2

Raw sequencing reads were trimmed using Cutadapt version 3.4 (Martin 2011), and pairs of reads shorter than 60bp after trimming were removed. Mitochondrial reads were also removed. McClintock v2.0.0 (Nelson et al. 2017) was run using default parameters. The *S. cerevisiae* reference genome file was downloaded from SGD (Engel et al. 2022). Of the suite of tools available through McClintock we found that RelocaTE2 (Chen et al. 2017) performed best against a subset of manually curated Ty insertions, so RelocaTE2 outputs were used for further analysis. Insertion locations given in the RelocaTE2 output file were then mapped back to the S288C reference genome to determine what genetic feature the insertion was in (‘gene', 'tRNA_gene', 'snoRNA_gene', 'snRNA_gene', 'long_terminal_repeat', 'transposable_element_gene'). The distance from each insertion location to the closest downstream tRNA was calculated. Alignments at all RelocaTE2 candidate Ty insertions were visually inspected and were used to curate the insertions.

All variants from both CLC Bio and relocaTE2 are available in Supplemental File 1, Supplemental File 2, Supplemental File 3, and Supplemental File 4.

Mutant strain re-barcoding

Evolved barcoded strains containing mutated alleles of *gat1*, *par32*, *mep1*, *mep2*, and *mep3* were crossed to GSY5936-5940 to replace the double barcode with the barcode landing pad able to accept new barcoding. Multiple MATalpha ura- segregants from the crosses were combined and transformed with pBAR3-L1 to generate double barcodes as described (Levy et al. 2015); multiple transformants were used to collect independently barcoded genotypes subsequently included in fitness remeasurements along with the original evolved strains.

Fitness re-measurement

To re-measure fitness, barcoded strains were grown in 100µL of YPD in microtiter plates and pooled. Pools were pre-grown in M14 or M3 medium (Levy et al. 2015), mixed with 10 volumes of culture of GSY5929 (wild type strain with digestible barcode) also pre-grown in M14 or M3 medium (time point 0 was taken right after mixing) and then passaged in triplicate through four batch transfers (400ul into 100ml of fresh M14 or M3 medium). 1.5mL of culture grown for 48 hours (time points 1, 2, 3 and 4) were used for DNA preparation using the YeaStar Genomic DNA kit (ZymoResearch D2002).

75ng of genomic DNA were used for PCR amplification in two 50µl reactions with 25µl 2xQ5 mix (NEB M0492), 2.5µM of each forward (FOS) and reverse (ROS) primers (Table S2) and water (to 50µl) for 22 cycles (care was taken to not overamplify the libraries). After amplification DNA was digested with ApaL1 enzyme overnight, run on a gel to select uncut PCR fragments (approximately 300bp) and purified from the gel using the QIAquick Gel Extraction Kit (Qiagen 28704). Individual libraries were quantified, mixed equimolarly and sequenced in

paired-end 300bp runs on MiSeq platform. Sequencing results were demultiplexed and resulting barcode frequencies were used to calculate the fitness as in (Blundell et al. 2019).

To measure fitness of the backcrossed and individually barcoded derivatives of selected adapted clones, the strains were pooled (including the parental strains remeasured above) and mixed with the GSY145 (wild type strain without an amplifiable barcode). After four batch transfers in M14 medium cells were collected, DNA was prepared and barcodes were amplified as above, except that individual PCR reactions were not digested, but instead were gel size selected in pools of six. Care was taken to not overamplify the libraries adjusting the cycle number for amplification.

Acknowledgements

The authors wish to thank Jamie Blundell for help with data analysis, and David Gresham, Frank Rosenzweig, and members of the Sherlock lab for helpful comments and discussions. Research reported in this publication was supported by the National Institute of Allergy and Infectious Diseases of the National Institutes of Health under Award Number F32AI160906 to MH. The content is solely the responsibility of the authors and does not necessarily represent the official views of the National Institutes of Health. MH was also supported by a Stanford Center for Computational Evolutionary and Human Genomics Postdoctoral fellowship and NIH NHGRI 5 T32 HG000044-24. DTS was supported by T32 GM00727646 and NSF GRFP DGE-1656518. The study was also funded by NIH grant R35 GM131824 to GS.

Data Availability

Whole genome sequencing data and barcode sequencing data for fitness remeasurement are available at the SRA under BioProject ID PRJNA882934.

References

Abdul-Rahman F, Tranchina D, Gresham D. 2021. Fluctuating Environments Maintain Genetic Diversity through Neutral Fitness Effects and Balancing Selection. *Mol Biol Evol* **38**: 4362-4375.

Ahn HW, Tucker JM, Arribere JA, Garfinkel DJ. 2017. Ribosome Biogenesis Modulates Ty1 Copy Number Control in Saccharomyces cerevisiae. *Genetics* **207**: 1441-1456.

Andre B. 1995. An overview of membrane transport proteins in Saccharomyces cerevisiae. *Yeast* **11**: 1575-1611.

Bleykasten-Grosshans C, Fabrizio R, Friedrich A, Schacherer J. 2021. Species-Wide Transposable Element Repertoires Retrace the Evolutionary History of the Saccharomyces cerevisiae Host. *Mol Biol Evol* **38**: 4334-4345.

Blundell JR, Schwartz K, Francois D, Fisher DS, Sherlock G, Levy SF. 2019. The dynamics of adaptive genetic diversity during the early stages of clonal evolution. *Nat Ecol Evol* **3**: 293-301.

Boeckstaens M, Andre B, Marini AM. 2007. The yeast ammonium transport protein Mep2 and its positive regulator, the Npr1 kinase, play an important role in normal and pseudohyphal growth on various nitrogen media through retrieval of excreted ammonium. *Mol Microbiol* **64**: 534-546.

Boeckstaens M, Merhi A, Llinares E, Van Vooren P, Springael JY, Wintjens R, Marini AM. 2015. Identification of a Novel Regulatory Mechanism of Nutrient Transport Controlled by TORC1-Npr1-Amu1/Par32. *PLoS Genet* **11**: e1005382.

Bonnet A, Lesage P. 2021. Light and shadow on the mechanisms of integration site selection in yeast Ty retrotransposon families. *Curr Genet* **67**: 347-357.

Bradshaw VA, McEntee K. 1989. DNA damage activates transcription and transposition of yeast Ty retrotransposons. *Mol Gen Genet* **218**: 465-474.

Brown CJ, Todd KM, Rosenzweig RF. 1998. Multiple duplications of yeast hexose transport genes in response to selection in a glucose-limited environment. *Mol Biol Evol* **15**: 931-942.

Chen D, Toone WM, Mata J, Lyne R, Burns G, Kivinen K, Brazma A, Jones N, Bahler J. 2003. Global transcriptional responses of fission yeast to environmental stress. *Mol Biol Cell* **14**: 214-229.

Chen J, Wrightsman TR, Wessler SR, Stajich JE. 2017. RelocaTE2: a high resolution transposable element insertion site mapping tool for population resequencing. *PeerJ* **5**: e2942.

Chenais B, Caruso A, Hiard S, Casse N. 2012. The impact of transposable elements on eukaryotic genomes: from genome size increase to genetic adaptation to stressful environments. *Gene* **509**: 7-15.

Coffman JA, Rai R, Loprete DM, Cunningham T, Svetlov V, Cooper TG. 1997. Cross regulation of four GATA factors that control nitrogen catabolic gene expression in Saccharomyces cerevisiae. *J Bacteriol* **179**: 3416-3429.

Company M, Adler C, Errede B. 1988. Identification of a Ty1 regulatory sequence responsive to STE7 and STE12. *Mol Cell Biol* **8**: 2545-2554.

Conrad M, Schothorst J, Kankipati HN, Van Zeebroeck G, Rubio-Texeira M, Thevelein JM. 2014. Nutrient sensing and signaling in the yeast Saccharomyces cerevisiae. *FEMS Microbiol Rev* **38**: 254-299.

Conte D, Jr., Barber E, Banerjee M, Garfinkel DJ, Curcio MJ. 1998. Posttranslational regulation of Ty1 retrotransposition by mitogen-activated protein kinase Fus3. *Mol Cell Biol* **18**: 2502-2513.

Cooper TG. 2002. Transmitting the signal of excess nitrogen in Saccharomyces cerevisiae from the Tor proteins to the GATA factors: connecting the dots. *FEMS Microbiol Rev* **26**: 223-238.

Cooper VS. 2018. Experimental Evolution as a High-Throughput Screen for Genetic Adaptations. *mSphere* **3**.

Curcio MJ, Hedge AM, Boeke JD, Garfinkel DJ. 1990. Ty RNA levels determine the spectrum of retrotransposition events that activate gene expression in Saccharomyces cerevisiae. *Mol Gen Genet* **220**: 213-221.

Czaja W, Bensasson D, Ahn HW, Garfinkel DJ, Bergman CM. 2020. Evolution of Ty1 copy number control in yeast by horizontal transfer and recombination. *PLoS Genet* **16**: e1008632.

Dan L, Li Y, Chen S, Liu J, Wang Y, Li F, He X, Carey LB. 2021. A rapidly reversible mutation generates subclonal genetic diversity and unstable drug resistance. *Proc Natl Acad Sci U S A* **118**.

Devine SE, Boeke JD. 1996. Integration of the yeast retrotransposon Ty1 is targeted to regions upstream of genes transcribed by RNA polymerase III. *Genes Dev* **10**: 620-633.

Engel SR, Wong ED, Nash RS, Aleksander S, Alexander M, Douglass E, Karra K, Miyasato SR, Simison M, Skrzypek MS et al. 2022. New data and collaborations at the Saccharomyces Genome Database: updated reference genome, alleles, and the Alliance of Genome Resources. *Genetics* **220**.

Esnault C, Lee M, Ham C, Levin HL. 2019. Transposable element insertions in fission yeast drive adaptation to environmental stress. *Genome Res* **29**: 85-95.

Ferreira T, Brethes D, Pinson B, Napias C, Chevallier J. 1997. Functional analysis of mutated purine-cytosine permease from Saccharomyces cerevisiae. A possible role of the hydrophilic segment 371-377 in the active carrier conformation. *J Biol Chem* **272**: 9697-9702.

Ferreira T, Chevallier J, Paumard P, Napias C, Brethes D. 1999. Screening of an intragenic second-site suppressor of purine-cytosine permease from Saccharomyces cerevisiae. Possible role of Ser272 in the base translocation process. *Eur J Biochem* **260**: 22-30.

Fouche S, Badet T, Oggenfuss U, Plissonneau C, Francisco CS, Croll D. 2020. Stress-Driven Transposable Element De-repression Dynamics and Virulence Evolution in a Fungal Pathogen. *Mol Biol Evol* **37**: 221-239.

Galhardo RS, Hastings PJ, Rosenberg SM. 2007. Mutation as a stress response and the regulation of evolvability. *Crit Rev Biochem Mol Biol* **42**: 399-435.

Garrett JM. 2008. Amino acid transport through the Saccharomyces cerevisiae Gap1 permease is controlled by the Ras/cAMP pathway. *Int J Biochem Cell Biol* **40**: 496-502.

Georis I, Feller A, Vierendeels F, Dubois E. 2009. The yeast GATA factor Gat1 occupies a central position in nitrogen catabolite repression-sensitive gene activation. *Mol Cell Biol* **29**: 3803-3815.

Good BH, McDonald MJ, Barrick JE, Lenski RE, Desai MM. 2017. The dynamics of molecular evolution over 60,000 generations. *Nature* **551**: 45-50.

Gresham D, Desai MM, Tucker CM, Jenq HT, Pai DA, Ward A, DeSevo CG, Botstein D, Dunham MJ. 2008. The repertoire and dynamics of evolutionary adaptations to controlled nutrient-limited environments in yeast. *PLoS Genet* **4**: e1000303.

Gresham D, Dunham MJ. 2014. The enduring utility of continuous culturing in experimental evolution. *Genomics* **104**: 399-405.
Gresham D, Hong J. 2015. The functional basis of adaptive evolution in chemostats. *FEMS Microbiol Rev* **39**: 2-16.
Gresham D, Usaite R, Germann SM, Lisby M, Botstein D, Regenberg B. 2010. Adaptation to diverse nitrogen-limited environments by deletion or extrachromosomal element formation of the GAP1 locus. *Proc Natl Acad Sci U S A* **107**: 18551-18556.
Haig D. 2016. Transposable elements: Self-seekers of the germline, team-players of the soma. *Bioessays* **38**: 1158-1166.
Hashida SN, Kitamura K, Mikami T, Kishima Y. 2003. Temperature shift coordinately changes the activity and the methylation state of transposon Tam3 in Antirrhinum majus. *Plant Physiol* **132**: 1207-1216.
Hashida SN, Uchiyama T, Martin C, Kishima Y, Sano Y, Mikami T. 2006. The temperature-dependent change in methylation of the Antirrhinum transposon Tam3 is controlled by the activity of its transposase. *Plant Cell* **18**: 104-118.
Hofman-Bang J. 1999. Nitrogen catabolite repression in Saccharomyces cerevisiae. *Mol Biotechnol* **12**: 35-73.
Hong J, Brandt N, Abdul-Rahman F, Yang A, Hughes T, Gresham D. 2018. An incoherent feedforward loop facilitates adaptive tuning of gene expression. *Elife* **7**.
Hong J, Gresham D. 2014. Molecular specificity, convergence and constraint shape adaptive evolution in nutrient-poor environments. *PLoS Genet* **10**: e1004041.
Hopkins P, Shaw R, Acik L, Oliver S, Eddy AA. 1992. Fluorocytosine causes uncoupled dissipation of the proton gradient and behaves as an imperfect substrate of the yeast cytosine permease. *Yeast* **8**: 1053-1064.
Jacquier H, Birgy A, Le Nagard H, Mechulam Y, Schmitt E, Glodt J, Bercot B, Petit E, Poulain J, Barnaud G et al. 2013. Capturing the mutational landscape of the beta-lactamase TEM-1. *Proc Natl Acad Sci U S A* **110**: 13067-13072.
Jardim SS, Schuch AP, Pereira CM, Loreto EL. 2015. Effects of heat and UV radiation on the mobilization of transposon mariner-Mos1. *Cell Stress Chaperones* **20**: 843-851.
Kao KC, Sherlock G. 2008. Molecular characterization of clonal interference during adaptive evolution in asexual populations of Saccharomyces cerevisiae. *Nat Genet* **40**: 1499-1504.
Kryazhimskiy S, Rice DP, Jerison ER, Desai MM. 2014. Microbial evolution. Global epistasis makes adaptation predictable despite sequence-level stochasticity. *Science* **344**: 1519-1522.
Kumaran R, Yang SY, Leu JY. 2013. Characterization of chromosome stability in diploid, polyploid and hybrid yeast cells. *PLoS One* **8**: e68094.
Kurtz JE, Exinger F, Erbs P, Jund R. 1999. New insights into the pyrimidine salvage pathway of Saccharomyces cerevisiae: requirement of six genes for cytidine metabolism. *Curr Genet* **36**: 130-136.
Kvitek DJ, Sherlock G. 2013. Whole genome, whole population sequencing reveals that loss of signaling networks is the major adaptive strategy in a constant environment. *PLoS Genet* **9**: e1003972.
Kwiatkowski TJ, Jr., Zoghbi HY, Ledbetter SA, Ellison KA, Chinault AC. 1990. Rapid identification of yeast artificial chromosome clones by matrix pooling and crude lysate PCR. *Nucleic Acids Res* **18**: 7191-7192.
Laloux I, Dubois E, Dewerchin M, Jacobs E. 1990. TEC1, a gene involved in the activation of Ty1 and Ty1-mediated gene expression in Saccharomyces cerevisiae: cloning and molecular analysis. *Mol Cell Biol* **10**: 3541-3550.
Laloux I, Jacobs E, Dubois E. 1994. Involvement of SRE element of Ty1 transposon in TEC1-dependent transcriptional activation. *Nucleic Acids Res* **22**: 999-1005.

Lang GI, Murray AW. 2008. Estimating the per-base-pair mutation rate in the yeast Saccharomyces cerevisiae. *Genetics* **178**: 67-82.
Lang GI, Rice DP, Hickman MJ, Sodergren E, Weinstock GM, Botstein D, Desai MM. 2013. Pervasive genetic hitchhiking and clonal interference in forty evolving yeast populations. *Nature* **500**: 571-574.
Lauer S, Avecilla G, Spealman P, Sethia G, Brandt N, Levy SF, Gresham D. 2018. Single-cell copy number variant detection reveals the dynamics and diversity of adaptation. *PLoS Biol* **16**: e3000069.
Lesage P, Todeschini AL. 2005. Happy together: the life and times of Ty retrotransposons and their hosts. *Cytogenet Genome Res* **110**: 70-90.
Levin HL, Moran JV. 2011. Dynamic interactions between transposable elements and their hosts. *Nat Rev Genet* **12**: 615-627.
Levy SF, Blundell JR, Venkataram S, Petrov DA, Fisher DS, Sherlock G. 2015. Quantitative evolutionary dynamics using high-resolution lineage tracking. *Nature* **519**: 181-186.
Li Y, Venkataram S, Agarwala A, Dunn B, Petrov DA, Sherlock G, Fisher DS. 2018. Hidden Complexity of Yeast Adaptation under Simple Evolutionary Conditions. *Curr Biol* **28**: 515-525 e516.
Long A, Liti G, Luptak A, Tenaillon O. 2015. Elucidating the molecular architecture of adaptation via evolve and resequence experiments. *Nat Rev Genet* **16**: 567-582.
Magasanik B, Kaiser CA. 2002. Nitrogen regulation in Saccharomyces cerevisiae. *Gene* **290**: 1-18.
Marini AM, Soussi-Boudekou S, Vissers S, Andre B. 1997. A family of ammonium transporters in Saccharomyces cerevisiae. *Mol Cell Biol* **17**: 4282-4293.
Martin M. 2011. Cutadapt removes adapter sequences from high-throughput sequencing reads. *EMBnetjournal* **17**.
Maxwell PH. 2020. Diverse transposable element landscapes in pathogenic and nonpathogenic yeast models: the value of a comparative perspective. *Mob DNA* **11**: 16.
Miousse IR, Chalbot MC, Lumen A, Ferguson A, Kavouras IG, Koturbash I. 2015. Response of transposable elements to environmental stressors. *Mutat Res Rev Mutat Res* **765**: 19-39.
Morillon A, Benard L, Springer M, Lesage P. 2002. Differential effects of chromatin and Gcn4 on the 50-fold range of expression among individual yeast Ty1 retrotransposons. *Mol Cell Biol* **22**: 2078-2088.
Morillon A, Springer M, Lesage P. 2000. Activation of the Kss1 invasive-filamentous growth pathway induces Ty1 transcription and retrotransposition in Saccharomyces cerevisiae. *Mol Cell Biol* **20**: 5766-5776.
Mularoni L, Zhou Y, Bowen T, Gangadharan S, Wheelan SJ, Boeke JD. 2012. Retrotransposon Ty1 integration targets specifically positioned asymmetric nucleosomal DNA segments in tRNA hotspots. *Genome Res* **22**: 693-703.
Nelson MG, Linheiro RS, Bergman CM. 2017. McClintock: An Integrated Pipeline for Detecting Transposable Element Insertions in Whole-Genome Shotgun Sequencing Data. *G3 (Bethesda)* **7**: 2763-2778.
Nishida Y, Pachulska-Wieczorek K, Blaszczyk L, Saha A, Gumna J, Garfinkel DJ, Purzycka KJ. 2015. Ty1 retrovirus-like element Gag contains overlapping restriction factor and nucleic acid chaperone functions. *Nucleic Acids Res* **43**: 7414-7431.
Ottaviani D, LeCain M, Sheer D. 2014. The role of microhomology in genomic structural variation. *Trends Genet* **30**: 85-94.
Payen C, Di Rienzi SC, Ong GT, Pogachar JL, Sanchez JC, Sunshine AB, Raghuraman MK, Brewer BJ, Dunham MJ. 2014. The dynamics of diverse segmental amplifications in populations of Saccharomyces cerevisiae adapting to strong selection. *G3 (Bethesda)* **4**: 399-409.

Payen C, Sunshine AB, Ong GT, Pogachar JL, Zhao W, Dunham MJ. 2016. High-Throughput Identification of Adaptive Mutations in Experimentally Evolved Yeast Populations. *PLoS Genet* **12**: e1006339.

Quinto-Alemany D, Canerina-Amaro A, Hernandez-Abad LG, Machin F, Romesberg FE, Gil-Lamaignere C. 2012. Yeasts acquire resistance secondary to antifungal drug treatment by adaptive mutagenesis. *PLoS One* **7**: e42279.

Ram Y, Hadany L. 2014. Stress-induced mutagenesis and complex adaptation. *Proc Biol Sci* **281**.

Regenberg B, During-Olsen L, Kielland-Brandt MC, Holmberg S. 1999. Substrate specificity and gene expression of the amino-acid permeases in Saccharomyces cerevisiae. *Curr Genet* **36**: 317-328.

Roquis D, Robertson M, Yu L, Thieme M, Julkowska M, Bucher E. 2021. Genomic impact of stress-induced transposable element mobility in Arabidopsis. *Nucleic Acids Res* **49**: 10431-10447.

Rowley PA. 2017. The frenemies within: viruses, retrotransposons and plasmids that naturally infect Saccharomyces yeasts. *Yeast* **34**: 279-292.

Rutherford JC, Chua G, Hughes T, Cardenas ME, Heitman J. 2008. A Mep2-dependent transcriptional profile links permease function to gene expression during pseudohyphal growth in Saccharomyces cerevisiae. *Mol Biol Cell* **19**: 3028-3039.

Sacerdot C, Mercier G, Todeschini AL, Dutreix M, Springer M, Lesage P. 2005. Impact of ionizing radiation on the life cycle of Saccharomyces cerevisiae Ty1 retrotransposon. *Yeast* **22**: 441-455.

Saha A, Mitchell JA, Nishida Y, Hildreth JE, Ariberre JA, Gilbert WV, Garfinkel DJ. 2015. A trans-dominant form of Gag restricts Ty1 retrotransposition and mediates copy number control. *J Virol* **89**: 3922-3938.

Sanchez MR, Miller AW, Liachko I, Sunshine AB, Lynch B, Huang M, Alcantara E, DeSevo CG, Pai DA, Tucker CM et al. 2017. Differential paralog divergence modulates genome evolution across yeast species. *PLoS Genet* **13**: e1006585.

Scholes DT, Banerjee M, Bowen B, Curcio MJ. 2001. Multiple regulators of Ty1 transposition in Saccharomyces cerevisiae have conserved roles in genome maintenance. *Genetics* **159**: 1449-1465.

Scholes DT, Kenny AE, Gamache ER, Mou Z, Curcio MJ. 2003. Activation of a LTR-retrotransposon by telomere erosion. *Proc Natl Acad Sci U S A* **100**: 15736-15741.

Sehgal A, Lee CY, Espenshade PJ. 2007. SREBP controls oxygen-dependent mobilization of retrotransposons in fission yeast. *PLoS Genet* **3**: e131.

Servant G, Pennetier C, Lesage P. 2008. Remodeling yeast gene transcription by activating the Ty1 long terminal repeat retrotransposon under severe adenine deficiency. *Mol Cell Biol* **28**: 5543-5554.

Servant G, Pinson B, Tchalikian-Cosson A, Coulpier F, Lemoine S, Pennetier C, Bridier-Nahmias A, Todeschini AL, Fayol H, Daignan-Fornier B et al. 2012. Tye7 regulates yeast Ty1 retrotransposon sense and antisense transcription in response to adenylic nucleotides stress. *Nucleic Acids Res* **40**: 5271-5282.

Spealman P, Burrell J, Gresham D. 2020. Inverted duplicate DNA sequences increase translocation rates through sequencing nanopores resulting in reduced base calling accuracy. *Nucleic Acids Res* **48**: 4940-4945.

Staleva Staleva L, Venkov P. 2001. Activation of Ty transposition by mutagens. *Mutat Res* **474**: 93-103.

Stoycheva T, Pesheva M, Venkov P. 2010. The role of reactive oxygen species in the induction of Ty1 retrotransposition in Saccharomyces cerevisiae. *Yeast* **27**: 259-267.

Todeschini AL, Morillon A, Springer M, Lesage P. 2005. Severe adenine starvation activates Ty1 transcription and retrotransposition in Saccharomyces cerevisiae. *Mol Cell Biol* **25**: 7459-7472.

Tucker JM, Larango ME, Wachsmuth LP, Kannan N, Garfinkel DJ. 2015. The Ty1 Retrotransposon Restriction Factor p22 Targets Gag. *PLoS Genet* **11**: e1005571.

Venkataram S, Dunn B, Li Y, Agarwala A, Chang J, Ebel ER, Geiler-Samerotte K, Herissant L, Blundell JR, Levy SF et al. 2016. Development of a Comprehensive Genotype-to-Fitness Map of Adaptation-Driving Mutations in Yeast. *Cell* **166**: 1585-1596 e1522.

Voordeckers K, Verstrepen KJ. 2015. Experimental evolution of the model eukaryote Saccharomyces cerevisiae yields insight into the molecular mechanisms underlying adaptation. *Curr Opin Microbiol* **28**: 1-9.

Wagner R, Straub ML, Souciet JL, Potier S, de Montigny J. 2001. New plasmid system to select for Saccharomyces cerevisiae purine-cytosine permease affinity mutants. *J Bacteriol* **183**: 4386-4388.

Wenger JW, Piotrowski J, Nagarajan S, Chiotti K, Sherlock G, Rosenzweig F. 2011. Hunger artists: yeast adapted to carbon limitation show trade-offs under carbon sufficiency. *PLoS Genet* **7**: e1002202.

Wilke CM, Adams J. 1992. Fitness effects of Ty transposition in Saccharomyces cerevisiae. *Genetics* **131**: 31-42.

Xu Z, Wei W, Gagneur J, Perocchi F, Clauder-Munster S, Camblong J, Guffanti E, Stutz F, Huber W, Steinmetz LM. 2009. Bidirectional promoters generate pervasive transcription in yeast. *Nature* **457**: 1033-1037.

Zhu YO, Siegal ML, Hall DW, Petrov DA. 2014. Precise estimates of mutation rate and spectrum in yeast. *Proc Natl Acad Sci U S A* **111**: E2310-2318.

Table S1. Primers used for Multiplexed barcode sequencing

F1	ACACTCTTTCCCTACACGACGCTCTTCCGATCTAACACCTATTAATATGGACTAAAGGAGGCTTTT
F2	ACACTCTTTCCCTACACGACGCTCTTCCGATCTACTAACTGTTAATATGGACTAAAGGAGGCTTTT
F3	ACACTCTTTCCCTACACGACGCTCTTCCGATCTATCGCCAGTTAATATGGACTAAAGGAGGCTTTT
F4	ACACTCTTTCCCTACACGACGCTCTTCCGATCTCATTCCAATTAATATGGACTAAAGGAGGCTTTT
F5	ACACTCTTTCCCTACACGACGCTCTTCCGATCTCGCATTAATTAATATGGACTAAAGGAGGCTTTT
F6	ACACTCTTTCCCTACACGACGCTCTTCCGATCTCTTCGCGCTTAATATGGACTAAAGGAGGCTTTT
F7	ACACTCTTTCCCTACACGACGCTCTTCCGATCTACGTAGCTTTAATATGGACTAAAGGAGGCTTTT
F8	ACACTCTTTCCCTACACGACGCTCTTCCGATCTATCCTATTTTAATATGGACTAAAGGAGGCTTTT
F9	ACACTCTTTCCCTACACGACGCTCTTCCGATCTCAGGAGGCTTAATATGGACTAAAGGAGGCTTTT
F10	ACACTCTTTCCCTACACGACGCTCTTCCGATCTCGACTGGGTTAATATGGACTAAAGGAGGCTTTT
F11	ACACTCTTTCCCTACACGACGCTCTTCCGATCTCTTAAGATTTAATATGGACTAAAGGAGGCTTTT
F12	ACACTCTTTCCCTACACGACGCTCTTCCGATCTGCAAGTAGTTAATATGGACTAAAGGAGGCTTTT
F13	ACACTCTTTCCCTACACGACGCTCTTCCGATCTATATAGGATTAATATGGACTAAAGGAGGCTTTT
F14	ACACTCTTTCCCTACACGACGCTCTTCCGATCTCACGTGTTTTAATATGGACTAAAGGAGGCTTTT
F15	ACACTCTTTCCCTACACGACGCTCTTCCGATCTCGAACTGTTTAATATGGACTAAAGGAGGCTTTT
F16	ACACTCTTTCCCTACACGACGCTCTTCCGATCTCTCTGTCTTTAATATGGACTAAAGGAGGCTTTT
F17	ACACTCTTTCCCTACACGACGCTCTTCCGATCTGATGGAATTTAATATGGACTAAAGGAGGCTTTT
F18	ACACTCTTTCCCTACACGACGCTCTTCCGATCTGGCAGACGTTAATATGGACTAAAGGAGGCTTTT
F19	ACACTCTTTCCCTACACGACGCTCTTCCGATCTCACAGTTGTTAATATGGACTAAAGGAGGCTTTT
F20	ACACTCTTTCCCTACACGACGCTCTTCCGATCTCCTTTACATTAATATGGACTAAAGGAGGCTTTT
F21	ACACTCTTTCCCTACACGACGCTCTTCCGATCTCTAGTCATTTAATATGGACTAAAGGAGGCTTTT
F22	ACACTCTTTCCCTACACGACGCTCTTCCGATCTGATCCAGCTTAATATGGACTAAAGGAGGCTTTT
F23	ACACTCTTTCCCTACACGACGCTCTTCCGATCTGGATATGGTTAATATGGACTAAAGGAGGCTTTT
F24	ACACTCTTTCCCTACACGACGCTCTTCCGATCTGTGACTACTTAATATGGACTAAAGGAGGCTTTT
F25	ACACTCTTTCCCTACACGACGCTCTTCCGATCTCCTACAACTTAATATGGACTAAAGGAGGCTTTT
F26	ACACTCTTTCCCTACACGACGCTCTTCCGATCTCTAGATTCTTAATATGGACTAAAGGAGGCTTTT
F27	ACACTCTTTCCCTACACGACGCTCTTCCGATCTGAGTTAACTTAATATGGACTAAAGGAGGCTTTT
F28	ACACTCTTTCCCTACACGACGCTCTTCCGATCTGGACGAGATTAATATGGACTAAAGGAGGCTTTT
F29	ACACTCTTTCCCTACACGACGCTCTTCCGATCTGTCTACATTTAATATGGACTAAAGGAGGCTTTT
F30	ACACTCTTTCCCTACACGACGCTCTTCCGATCTTATACCGTTTAATATGGACTAAAGGAGGCTTTT
F31	ACACTCTTTCCCTACACGACGCTCTTCCGATCTCGTCGGCTTTAATATGGACTAAAGGAGGCTTTT
F32	ACACTCTTTCCCTACACGACGCTCTTCCGATCTGAGAACTCTTAATATGGACTAAAGGAGGCTTTT
F33	ACACTCTTTCCCTACACGACGCTCTTCCGATCTGCTGGCGATTAATATGGACTAAAGGAGGCTTTT
F34	ACACTCTTTCCCTACACGACGCTCTTCCGATCTGTCCATTATTAATATGGACTAAAGGAGGCTTTT
F35	ACACTCTTTCCCTACACGACGCTCTTCCGATCTTAGTCACATTAATATGGACTAAAGGAGGCTTTT
F36	ACACTCTTTCCCTACACGACGCTCTTCCGATCTTGACGCATTTAATATGGACTAAAGGAGGCTTTT
F37	ACACTCTTTCCCTACACGACGCTCTTCCGATCTGACGTCAATTAATATGGACTAAAGGAGGCTTTT
F38	ACACTCTTTCCCTACACGACGCTCTTCCGATCTGCTCAGTTTTAATATGGACTAAAGGAGGCTTTT
F39	ACACTCTTTCCCTACACGACGCTCTTCCGATCTGTAGAGCTTTAATATGGACTAAAGGAGGCTTTT
F40	ACACTCTTTCCCTACACGACGCTCTTCCGATCTTAGCTAGTTTAATATGGACTAAAGGAGGCTTTT
F41	ACACTCTTTCCCTACACGACGCTCTTCCGATCTTGAATTCGTTAATATGGACTAAAGGAGGCTTTT
F42	ACACTCTTTCCCTACACGACGCTCTTCCGATCTTTCCTCACTTAATATGGACTAAAGGAGGCTTTT
F43	ACACTCTTTCCCTACACGACGCTCTTCCGATCTGCGTTTCGTTAATATGGACTAAAGGAGGCTTTT
F44	ACACTCTTTCCCTACACGACGCTCTTCCGATCTGTACTTGCTTAATATGGACTAAAGGAGGCTTTT
F45	ACACTCTTTCCCTACACGACGCTCTTCCGATCTTACTGCGCTTAATATGGACTAAAGGAGGCTTTT
F46	ACACTCTTTCCCTACACGACGCTCTTCCGATCTTCGGTACCTTAATATGGACTAAAGGAGGCTTTT
F47	ACACTCTTTCCCTACACGACGCTCTTCCGATCTTTAAACAGTTAATATGGACTAAAGGAGGCTTTT
F48	ACACTCTTTCCCTACACGACGCTCTTCCGATCTAATGCTGATTAATATGGACTAAAGGAGGCTTTT
F49	ACACTCTTTCCCTACACGACGCTCTTCCGATCTGGTCTGACTTAATATGGACTAAAGGAGGCTTTT
F50	ACACTCTTTCCCTACACGACGCTCTTCCGATCTTACGAATCTTAATATGGACTAAAGGAGGCTTTT

F51	ACACTCTTTCCCTACACGACGCTCTTCCGATCTTCGCGTACTTAATATGGACTAAAGGAGGCTTTT
F52	ACACTCTTTCCCTACACGACGCTCTTCCGATCTTGTGCTATTTAATATGGACTAAAGGAGGCTTTT
F53	ACACTCTTTCCCTACACGACGCTCTTCCGATCTAATCACACTTAATATGGACTAAAGGAGGCTTTT
F54	ACACTCTTTCCCTACACGACGCTCTTCCGATCTAGGTCAGTTTAATATGGACTAAAGGAGGCTTTT
F55	ACACTCTTTCCCTACACGACGCTCTTCCGATCTGTTTCACTTTAATATGGACTAAAGGAGGCTTTT
F56	ACACTCTTTCCCTACACGACGCTCTTCCGATCTTCCTACTATTAATATGGACTAAAGGAGGCTTTT
F57	ACACTCTTTCCCTACACGACGCTCTTCCGATCTTGTAGGTCTTAATATGGACTAAAGGAGGCTTTT
F58	ACACTCTTTCCCTACACGACGCTCTTCCGATCTAAGATTGCTTAATATGGACTAAAGGAGGCTTTT
F59	ACACTCTTTCCCTACACGACGCTCTTCCGATCTAGGCAATGTTAATATGGACTAAAGGAGGCTTTT
F60	ACACTCTTTCCCTACACGACGCTCTTCCGATCTATTGCATCTTAATATGGACTAAAGGAGGCTTTT
F61	ACACTCTTTCCCTACACGACGCTCTTCCGATCTTCCAGCCTTTAATATGGACTAAAGGAGGCTTTT
F62	ACACTCTTTCCCTACACGACGCTCTTCCGATCTTGGTCTTCTTAATATGGACTAAAGGAGGCTTTT
F63	ACACTCTTTCCCTACACGACGCTCTTCCGATCTAAGCGGTCTTAATATGGACTAAAGGAGGCTTTT
F64	ACACTCTTTCCCTACACGACGCTCTTCCGATCTAGAACACCTTAATATGGACTAAAGGAGGCTTTT
F65	ACACTCTTTCCCTACACGACGCTCTTCCGATCTATGCATCCTTAATATGGACTAAAGGAGGCTTTT
F66	ACACTCTTTCCCTACACGACGCTCTTCCGATCTCCATACACTTAATATGGACTAAAGGAGGCTTTT
F67	ACACTCTTTCCCTACACGACGCTCTTCCGATCTTGCGGTTATTAATATGGACTAAAGGAGGCTTTT
F68	ACACTCTTTCCCTACACGACGCTCTTCCGATCTAACCGTGTTTAATATGGACTAAAGGAGGCTTTT
F69	ACACTCTTTCCCTACACGACGCTCTTCCGATCTACTCTAAGTTAATATGGACTAAAGGAGGCTTTT
F70	ACACTCTTTCCCTACACGACGCTCTTCCGATCTATGAGGAATTAATATGGACTAAAGGAGGCTTTT
F71	ACACTCTTTCCCTACACGACGCTCTTCCGATCTCCAGCACGTTAATATGGACTAAAGGAGGCTTTT
F72	ACACTCTTTCCCTACACGACGCTCTTCCGATCTCGCTTCTGTTAATATGGACTAAAGGAGGCTTTT
R1	CTCGGCATTCCTGCTGAACCGCTCTTCCGATCTTATCTCCGTCGAATTCAAGCTTAGATCTGATA
R2	CTCGGCATTCCTGCTGAACCGCTCTTCCGATCTTGATCCGATCGAATTCAAGCTTAGATCTGATA
R3	CTCGGCATTCCTGCTGAACCGCTCTTCCGATCTAGTAGTGGTCGAATTCAAGCTTAGATCTGATA
R4	CTCGGCATTCCTGCTGAACCGCTCTTCCGATCTCAATCATCTCGAATTCAAGCTTAGATCTGATA
R5	CTCGGCATTCCTGCTGAACCGCTCTTCCGATCTGAACGCTGTCGAATTCAAGCTTAGATCTGATA
R6	CTCGGCATTCCTGCTGAACCGCTCTTCCGATCTGCGGCGAATCGAATTCAAGCTTAGATCTGATA
R7	CTCGGCATTCCTGCTGAACCGCTCTTCCGATCTGTGGGATATCGAATTCAAGCTTAGATCTGATA
R8	CTCGGCATTCCTGCTGAACCGCTCTTCCGATCTTCATTAGGTCGAATTCAAGCTTAGATCTGATA
R9	CTCGGCATTCCTGCTGAACCGCTCTTCCGATCTACAGTGCATCGAATTCAAGCTTAGATCTGATA
R10	CTCGGCATTCCTGCTGAACCGCTCTTCCGATCTAGTTGCTATCGAATTCAAGCTTAGATCTGATA
R11	CTCGGCATTCCTGCTGAACCGCTCTTCCGATCTCGGACGTGTCGAATTCAAGCTTAGATCTGATA
R12	CTCGGCATTCCTGCTGAACCGCTCTTCCGATCTGACACTCTTCGAATTCAAGCTTAGATCTGATA
R13	CTCGGCATTCCTGCTGAACCGCTCTTCCGATCTGGCGAGGATCGAATTCAAGCTTAGATCTGATA
R14	CTCGGCATTCCTGCTGAACCGCTCTTCCGATCTGTTGTCCCTCGAATTCAAGCTTAGATCTGATA
R15	CTCGGCATTCCTGCTGAACCGCTCTTCCGATCTTTCTGATGTCGAATTCAAGCTTAGATCTGATA
R16	CTCGGCATTCCTGCTGAACCGCTCTTCCGATCTACCGTTATTCGAATTCAAGCTTAGATCTGATA
R17	CTCGGCATTCCTGCTGAACCGCTCTTCCGATCTCCGGATAGTCGAATTCAAGCTTAGATCTGATA
R18	CTCGGCATTCCTGCTGAACCGCTCTTCCGATCTCGGTTGATTCGAATTCAAGCTTAGATCTGATA
R19	CTCGGCATTCCTGCTGAACCGCTCTTCCGATCTGCAGCCTCTCGAATTCAAGCTTAGATCTGATA
R20	CTCGGCATTCCTGCTGAACCGCTCTTCCGATCTGGTCCTTGTCGAATTCAAGCTTAGATCTGATA
R21	CTCGGCATTCCTGCTGAACCGCTCTTCCGATCTTGAGAGTGTCGAATTCAAGCTTAGATCTGATA
R22	CTCGGCATTCCTGCTGAACCGCTCTTCCGATCTTTGAGTGTTCGAATTCAAGCTTAGATCTGATA
R23	CTCGGCATTCCTGCTGAACCGCTCTTCCGATCTCAAGACCATCGAATTCAAGCTTAGATCTGATA
R24	CTCGGCATTCCTGCTGAACCGCTCTTCCGATCTCCGTCTGATCGAATTCAAGCTTAGATCTGATA
R25	CTCGGCATTCCTGCTGAACCGCTCTTCCGATCTTGCGGTTATCGAATTCAAGCTTAGATCTGATA
R26	CTCGGCATTCCTGCTGAACCGCTCTTCCGATCTAACCGTGTTCGAATTCAAGCTTAGATCTGATA
R27	CTCGGCATTCCTGCTGAACCGCTCTTCCGATCTACTCTAAGTCGAATTCAAGCTTAGATCTGATA
R28	CTCGGCATTCCTGCTGAACCGCTCTTCCGATCTATGAGGAATCGAATTCAAGCTTAGATCTGATA
R29	CTCGGCATTCCTGCTGAACCGCTCTTCCGATCTCCAGCACGTCGAATTCAAGCTTAGATCTGATA
R30	CTCGGCATTCCTGCTGAACCGCTCTTCCGATCTCGCTTCTGTCGAATTCAAGCTTAGATCTGATA
R31	CTCGGCATTCCTGCTGAACCGCTCTTCCGATCTTCCAGCCTTCGAATTCAAGCTTAGATCTGATA
R32	CTCGGCATTCCTGCTGAACCGCTCTTCCGATCTTGGTCTTCTCGAATTCAAGCTTAGATCTGATA

R33	CTCGGCATTCCTGCTGAACCGCTCTTCCGATCTAAGCGGTCTCGAATTCAAGCTTAGATCTGATA
R34	CTCGGCATTCCTGCTGAACCGCTCTTCCGATCTAGAACACCTCGAATTCAAGCTTAGATCTGATA
R35	CTCGGCATTCCTGCTGAACCGCTCTTCCGATCTATGCATCCTCGAATTCAAGCTTAGATCTGATA
R36	CTCGGCATTCCTGCTGAACCGCTCTTCCGATCTCCATACACTCGAATTCAAGCTTAGATCTGATA
R37	CTCGGCATTCCTGCTGAACCGCTCTTCCGATCTGTTTCACTTCGAATTCAAGCTTAGATCTGATA
R38	CTCGGCATTCCTGCTGAACCGCTCTTCCGATCTTCCTACTATCGAATTCAAGCTTAGATCTGATA
R39	CTCGGCATTCCTGCTGAACCGCTCTTCCGATCTTGTAGGTCTCGAATTCAAGCTTAGATCTGATA
R40	CTCGGCATTCCTGCTGAACCGCTCTTCCGATCTAAGATTGCTCGAATTCAAGCTTAGATCTGATA
R41	CTCGGCATTCCTGCTGAACCGCTCTTCCGATCTAGGCAATGTCGAATTCAAGCTTAGATCTGATA
R42	CTCGGCATTCCTGCTGAACCGCTCTTCCGATCTATTGCATCTCGAATTCAAGCTTAGATCTGATA
R43	CTCGGCATTCCTGCTGAACCGCTCTTCCGATCTGACGTCAATCGAATTCAAGCTTAGATCTGATA
R44	CTCGGCATTCCTGCTGAACCGCTCTTCCGATCTGCTCAGTTTCGAATTCAAGCTTAGATCTGATA
R45	CTCGGCATTCCTGCTGAACCGCTCTTCCGATCTGTAGAGCTTCGAATTCAAGCTTAGATCTGATA
R46	CTCGGCATTCCTGCTGAACCGCTCTTCCGATCTTAGCTAGTTCGAATTCAAGCTTAGATCTGATA
R47	CTCGGCATTCCTGCTGAACCGCTCTTCCGATCTTGAATTCGTCGAATTCAAGCTTAGATCTGATA
R48	CTCGGCATTCCTGCTGAACCGCTCTTCCGATCTTTCCTCACTCGAATTCAAGCTTAGATCTGATA
R49	CTCGGCATTCCTGCTGAACCGCTCTTCCGATCTCGTCGGCTTCGAATTCAAGCTTAGATCTGATA
R50	CTCGGCATTCCTGCTGAACCGCTCTTCCGATCTGAGAACTCTCGAATTCAAGCTTAGATCTGATA
R51	CTCGGCATTCCTGCTGAACCGCTCTTCCGATCTGCTGGCGATCGAATTCAAGCTTAGATCTGATA
R52	CTCGGCATTCCTGCTGAACCGCTCTTCCGATCTGTCCATTATCGAATTCAAGCTTAGATCTGATA
R53	CTCGGCATTCCTGCTGAACCGCTCTTCCGATCTTAGTCACATCGAATTCAAGCTTAGATCTGATA
R54	CTCGGCATTCCTGCTGAACCGCTCTTCCGATCTTGACGCATTCGAATTCAAGCTTAGATCTGATA
R55	CTCGGCATTCCTGCTGAACCGCTCTTCCGATCTGGTCTGACTCGAATTCAAGCTTAGATCTGATA
R56	CTCGGCATTCCTGCTGAACCGCTCTTCCGATCTTACGAATCTCGAATTCAAGCTTAGATCTGATA
R57	CTCGGCATTCCTGCTGAACCGCTCTTCCGATCTTCGCGTACTCGAATTCAAGCTTAGATCTGATA
R58	CTCGGCATTCCTGCTGAACCGCTCTTCCGATCTTGTGCTATTCGAATTCAAGCTTAGATCTGATA
R59	CTCGGCATTCCTGCTGAACCGCTCTTCCGATCTAATCACACTCGAATTCAAGCTTAGATCTGATA
R60	CTCGGCATTCCTGCTGAACCGCTCTTCCGATCTAGGTCAGTTCGAATTCAAGCTTAGATCTGATA
R61	CTCGGCATTCCTGCTGAACCGCTCTTCCGATCTGCGTTTCGTCGAATTCAAGCTTAGATCTGATA
R62	CTCGGCATTCCTGCTGAACCGCTCTTCCGATCTGTACTTGCTCGAATTCAAGCTTAGATCTGATA
R63	CTCGGCATTCCTGCTGAACCGCTCTTCCGATCTTACTGCGCTCGAATTCAAGCTTAGATCTGATA
R64	CTCGGCATTCCTGCTGAACCGCTCTTCCGATCTTCGGTACCTCGAATTCAAGCTTAGATCTGATA

Table S2. Primers used for Barcode Amplification for Fitness Remeasurement

FOS1	AATGATACGGCGACCACCGAGATCTACACTCTTTCCCTACACGACGCTCTTCCGATCT TTAATATGGACTAAAGGAGGCTTTT
FOS2	AATGATACGGCGACCACCGAGATCTACACTCTTTCCCTACACGACGCTCTTCCGATCT TCGTTTAATATGGACTAAAGGAGGCTTTT
FOS3	AATGATACGGCGACCACCGAGATCTACACTCTTTCCCTACACGACGCTCTTCCGATCT CTTATTAATATGGACTAAAGGAGGCTTTT
FOS4	AATGATACGGCGACCACCGAGATCTACACTCTTTCCCTACACGACGCTCTTCCGATCT GCCGTTTAATATGGACTAAAGGAGGCTTTT
FOS5	AATGATACGGCGACCACCGAGATCTACACTCTTTCCCTACACGACGCTCTTCCGATCT ATGATTTAATATGGACTAAAGGAGGCTTTT
FOS6	AATGATACGGCGACCACCGAGATCTACACTCTTTCCCTACACGACGCTCTTCCGATCT ACTGCTTTAATATGGACTAAAGGAGGCTTTT
FOS7	AATGATACGGCGACCACCGAGATCTACACTCTTTCCCTACACGACGCTCTTCCGATCT CGTTGATTAATATGGACTAAAGGAGGCTTTT
FOS8	AATGATACGGCGACCACCGAGATCTACACTCTTTCCCTACACGACGCTCTTCCGATCT CAGCAGTTAATATGGACTAAAGGAGGCTTTT
FOS9	AATGATACGGCGACCACCGAGATCTACACTCTTTCCCTACACGACGCTCTTCCGATCT TTCAGCTTAATATGGACTAAAGGAGGCTTTT
FOS10	AATGATACGGCGACCACCGAGATCTACACTCTTTCCCTACACGACGCTCTTCCGATCT GTAACCTTAATATGGACTAAAGGAGGCTTTT
ROS1	CAAGCAGAAGACGGCATACGAGATCGGTCTCGGCATTCCTGCTGAACCGCTCTTCCGATCT TCGAATTCAAGCTTAGATCTGATA
ROS2	CAAGCAGAAGACGGCATACGAGATCGGTCTCGGCATTCCTGCTGAACCGCTCTTCCGATCT AGTCGAATTCAAGCTTAGATCTGATA
ROS3	CAAGCAGAAGACGGCATACGAGATCGGTCTCGGCATTCCTGCTGAACCGCTCTTCCGATCT CTTATCGAATTCAAGCTTAGATCTGATA
ROS4	CAAGCAGAAGACGGCATACGAGATCGGTCTCGGCATTCCTGCTGAACCGCTCTTCCGATCT GACTCGAATTCAAGCTTAGATCTGATA
ROS5	CAAGCAGAAGACGGCATACGAGATCGGTCTCGGCATTCCTGCTGAACCGCTCTTCCGATCT ACATCGAATTCAAGCTTAGATCTGATA
ROS6	CAAGCAGAAGACGGCATACGAGATCGGTCTCGGCATTCCTGCTGAACCGCTCTTCCGATCT CACGTCGAATTCAAGCTTAGATCTGATA

Supplemental Files

Supplemental File 1. All Variants identified in Nitrogen evolved clones

Supplemental File 2. Annotated output from RelocaTE2 for curated insertions from analyzing clones from Nitrogen evolution

Supplemental File 3. CLC Bio output for putative Ty insertion events in from analyzing clones from nitrogen evolution

Supplemental File 4. Annotated output from RelocaTE2 for curated insertions from analyzing clones from Venkataram et al.